Contents

目录

Abstract

摘要

We summarize our work on spherically symmetric midi-superspaces in loop quantum gravity. Our approach is based on using inhomogeneous slicings that may penetrate the horizon in case there is one and on a redefinition of the constraints so the Hamiltonian has an Abelian algebra with itself. We discuss basic and improved quantizations as is done in loop quantum cosmology. We discuss the use of parameterized Dirac observables to define operators associated with kinematical variables in the physical space of states, as a first step to introduce an operator associated with the space-time metric. We analyze the elimination of singularities and how they are replaced by extensions of the space-times. We discuss the charged case and potential observational consequences in quasinormal modes. We also analyze the covariance of the approach. Finally, we comment on other recent approaches of quantum black holes, including mini-superspaces motivated by loop quantum gravity.

我们总结了本人在圈量子引力中球对称 midi-超空间的研究工作。我们的方法基于两点: 一是使用可穿透事件视界 (若存在) 的非均匀切片，二是对约束条件重新定义，使哈密顿量自身对易，从而生成阿贝尔代数。我们参照圈量子宇宙学的思路，讨论了基础量子化与改进量子化两种方案。我们探讨了利用参数化狄拉克可观测量，在物理态空间中定义与运动学变量关联的算符，这是引入时空度量关联算符的第一步。我们分析了奇点的消除，以及奇点如何被延拓的时空所取代。我们讨论了带电线腔，以及拟正则模式的潜在观测效应。我们还分析了该方法的协变性。最后，我们评述了其他近期量子黑洞研究方案，包括由圈量子引力启发得到的迷你超空间相关研究。

R. Gambini

R. 甘比尼

Instituto de Física, Facultad de Ciencias, Universidad de la República, Montevideo, Uruguay e-mail: rgambini@fisica.edu.uy

乌拉圭蒙得维的亚共和国大学理学院物理研究所，电子邮箱:rgambini@fisica.edu.uy

J. Olmedo

J. 奥尔梅多

Departamento de Física Teórica y del Cosmos, Universidad de Granada, Granada, Spain e-mail: javolmedo@ugr.es

西班牙格拉纳达格拉纳达大学宇宙与理论物理系，电子邮箱:javolmedo@ugr.es

J. Pullin (☑)

J. 普林 (☑)

Department of Physics and Astronomy, Louisiana State University, Baton Rouge, LA, USA e-mail: pullin@lsu.edu

美国路易斯安那州巴吞鲁日路易斯安那州立大学物理与天文学系，电子邮箱:pullin@lsu.edu

Keywords

关键词

Spherical symmetry - Loop quantum gravity - Black holes - Singularity resolution

球对称 - 圈量子引力 - 黑洞 - 奇点消解

Introduction

引言

The study of situations of high symmetry in which one first applies the symmetry to the classical theory and then proceeds to quantize has proven a valuable tool to probe potential regimes of quantum gravity in a scenario where detailed, well-controlled, calculations are possible. A prime example of this is loop quantum cosmology (LQC) [1] where spatial homogeneity is imposed before quantization. It has led to several attractive insights like the elimination of the Big Bang singularity, even though it implies a radical reduction of the degrees of freedom of the theory (from infinitely many to a finite number). It is a natural progression to attempt to consider situations with less symmetry. In that context, spherically symmetric space-times appear as an attractive scenario since they include the important case of black holes. And although general relativity with spherical symmetry does not have field-theoretic degrees of freedom on-shell, initially the treatment resembles that of a situation with infinitely many degrees of freedom. In particular, the constraints of the theory do not form a Lie algebra, but an algebra with structure functions like in the full theory. This can be a significant impediment to complete the Dirac quantization of the theory, as there are several well-known obstacles that the structure functions introduce [2]. It therefore came as a welcome surprise when it was noted that a rescaling [3, 4] of the constraints can actually turn them into a Lie algebra. We are not aware of any deep reason for the emergence of this possibility for these models. In particular, it does not seem to survive

the inclusion of matter. But, nevertheless, it allows to complete the Dirac quantization and discuss interesting properties in the vacuum case.

研究高对称情形时，先对经典理论施加对称性约束再进行量子化，这一方法已被证明是研究量子引力可能能区的有效工具，能在该框架下完成细致可控的计算。圈量子宇宙学 (LQC)[1] 就是一个典型例子，它在量子化前先引入空间均匀性假设。尽管该假设大幅约化了理论的自由度 (从无穷多变为有限个)，但仍得到了若干引人关注的结论，例如消除了大爆炸奇点。自然地，人们接下来尝试研究对称性更低的情形。在此背景下，球对称时空是很有吸引力的研究框架，因为它包含了黑洞这一重要研究对象。虽然球对称广义相对论在壳没有场论自由度，但其初始处理过程仍然类似具有无穷多自由度的情形。特别地，该理论的约束不构成李代数，而是和完整理论一样，构成带有结构函数的代数。结构函数会带来若干广为人知的困难 [2]，这会对完成理论的狄拉克量子化构成重大阻碍。因此，当人们发现可以对约束做重标度 [3, 4] 将其转化为李代数时，这着实是一个惊喜。我们目前还不知道这类模型能出现这一性质的深层原因。尤其是引入物质后，这一性质似乎就无法保留。但尽管如此，在真空情形下，它仍能让我们完成狄拉克量子化，并讨论诸多有趣性质。

In this manuscript, we will review our work on spherical symmetry, which is based on the use of inhomogeneous slices that may penetrate horizons when they are present and become homogeneous inside. There are other approaches to spherical symmetry that focus on the interiors of black holes exploiting the isometry of the

在本文中，我们将回顾我们在球对称方向的研究工作，我们的工作基于非均匀切片的使用: 这类切片可以穿透存在的视界，并在视界内部变为均匀切片。

Schwarzschild interior with the Kantowski-Sachs space-times, and some consider extensions to the exterior. There is a significant literature on the subject (see [5] and references therein), and we will dedicate a section at the end of this chapter. A separate review of our work is present in [8].

史瓦西内部与坎托夫斯基-萨克斯时空具有等距性，现有其他研究球对称的方法利用该等距性聚焦于黑洞内部，也有部分工作考虑了对外部区域的拓展。关于该主题已有大量研究文献 (见 [5] 及其中参考文献)，我们会在本章末尾专门用一节讨论。我们另有一篇工作综述见 [8]。

New Variables for Gravity with Spherical Symmetry

球对称引力的新变量

Ashtekar's new variables cast general relativity in terms of quantities that resemble the variables of an $SU(2)$ Yang-Mills theory. Spherically symmetric configurations in that theory were already considered in the 1970s by Cordero and Teitelboim [6]. Their results can be adapted to the Ashtekar's variables context and were discussed in detail by Bojowald and Swiderski [7]. We will not conduct a full review of the spherical reduction here but just introduce the resulting variables and their connection to the traditional metric variables. One is left with a "radial" and "transverse" components of the triads E^x and E^φ , respectively. We call the radial variable x so as not to prejudice in terms of a particular radial coordinate like isotropic or Schwarzschild. Their canonically conjugate momenta are denoted by K_x and K_φ , respectively, with Poisson brackets,

阿西特卡新变量用类似 $SU(2)$ 杨-米尔斯理论的变量形式重构了广义相对论。该理论中的球对称构型早在 20 世纪 70 年代就由科尔德罗和泰特尔鲍姆研究过 [6]。他们的结果可以适配到阿西特卡变量框架下，且已由博约瓦尔德与斯威德斯基已对其做了详细讨论 [7]。本文不会在此对球约化做完整综述，仅介绍约化得到的变量及其与传统度规变量的联系。最终得到三元组 E^x 和 E^φ 分别为「径向」分量和「横向」分量。我们将径向变量称为 x，以避免限定在各向同性或史瓦西这类特定径向坐标。它们的正则共轭动量分别记为 K_x 和 K_φ，其泊松括号为，

$$\{K_x(x), E^x(\tilde{x})\} = G\delta(x-\tilde{x}),$$

$$\left\{K_\varphi(x), E^\varphi(\tilde{x})\right\} = G\delta(x-\tilde{x}), \tag{1}$$

with G Newton’s constant. We take the Immirzi parameter to 1 .

其中 G 是牛顿引力常数。我们取伊米尔齐参数为 1。

The relationship with the traditional metric variables is,

其与传统度规变量的关系为，

$$g_{xx} = \frac{(E^\varphi)^2}{|E^x|}, \tag{2}$$

$$g_{\theta\theta} = |E^x|, \tag{3}$$

$$K_{xx} = -\frac{2K_x(E^\varphi)}{\sqrt{|E^x|}}, \tag{4}$$

$$K_{\theta\theta} = -\sqrt{|E^x|}K_\varphi. \tag{5}$$

The use of symmetry-adapted variables obviously implies to work in a restricted set of coordinates (gauges). This eliminates the Gauss law usually present in the Ashtekar formulation. One is left with one diffeomorphism constraint in the radial variable and the Hamiltonian constraint. In terms of the variables we are considering, they take the form,

使用适配对称性的变量显然意味着我们在受限的坐标 (规范) 集合中工作。这消除了阿西特卡表述中通常存在的高斯定律。最终得到径向变量下的一个微分同胚约束和哈密顿约束。在我们研究的变量下，它们的形式为，

$$H_r := G^{-1}\left[E^\varphi K_\varphi' - (E^x)' K_x\right], \tag{6a}$$

$$H := G^{-1}\left\{\frac{\left[(E^x)'\right]^2}{8\sqrt{E^x}E^\varphi} - \frac{E^\varphi}{2\sqrt{E^x}} - 2K_\varphi\sqrt{E^x}K_x - \frac{E^\varphi K_\varphi^2}{2\sqrt{E^x}} - \frac{\sqrt{E^x}(E^x)'(E^\varphi)'}{2(E^\varphi)^2} + \frac{\sqrt{E^x}(E^x)''}{2E^\varphi}\right\}, \tag{6b}$$

where prime is derivative with respect to the radial coordinate x . These expressions are valid for $E^x > 0$. They can be extended to the full real axis substituting E^x by $|E^x|$. These constraints have the same algebra as in the full theory, in particular the Poisson brackets of two Hamiltonian constraints are proportional to the diffeomorphism constraint, and the proportionality factor is a structure function that involves the metric. It is therefore not a Lie algebra and faces the same wellknown difficulties about promoting it to a quantum algebra of self-adjoint operators as one has in the full theory we mentioned before [2].

其中撇号表示对径向坐标 x 求导。这些表达式对 $E^x > 0$ 成立。可以将其延拓到整个实轴，只需将 E^x 替换为 $|E^x|$ 即可。这些约束具有与完整理论相同的代数，具体来说，两个哈密顿约束的泊松括号与微分同胚约束成正比，比例系数是一个依赖度规的结构函数。因此这不是李代数，它面临着和我们前文提到的完整理论中相同的著名难题: 如何将其提升为自伴算子的量子代数 [2]。

It should be noted, however, that the variable K_x appears undifferentiated in both the Hamiltonian and diffeomorphism constraints. This suggests the possibility of eliminating it. So performing the linear combination,

但需要注意，变量 K_x 在哈密顿约束和微分同胚约束中都没有出现微分，这说明有可能消去它。因此我们做线性组合，

$$H_{\rm new} := \frac{(E^x)'}{E^\varphi} H - 2\frac{\sqrt{E^x}}{E^\varphi} K_\varphi H_r = -\frac{1}{G}\left[\sqrt{E^x}\left(1 - \frac{\left[(E^x)'\right]^2}{4(E^\varphi)^2} + K_\varphi^2\right)\right]', \tag{7}$$

one is left with a Hamiltonian constraint $H_{\rm new}$ that has vanishing Poisson bracket with itself and has the usual Hamiltonian/diffeomorphism Poisson bracket. The algebra of constraints therefore becomes a Lie algebra, opening the possibility of promoting the constraints to self-adjoint operators. The linear combination is equivalent to redefining the lapse and the shift,

最终得到哈密顿约束 $H_{\rm new}$ ，它与自身的泊松括号为零，且满足常规的哈密顿/微分同胚泊松括号。因此约束代数变为李代数，这为将约束提升为自伴算子打开了可能。该线性组合等价于重新定义流逝函数和位移，

$$N_r^{\rm new} := N_r - 2N\frac{K_\varphi\sqrt{E^x}}{(E^x)'},\ N_{\rm new} := N\frac{E^\varphi}{(E^x)'}. \tag{8}$$

We will find it more convenient to work with the smeared version of the Hamiltonian constraint. This requires some care with the falloff of the various quantities at the edges of the manifold considered. This was discussed by Kuchař [9] in terms of the traditional variables, and the use of the Ashtekar new variables does not add to this discussion (apart from changes in notation) so we will not repeat it here. Details can be found in [8]. The final result, after an integration by parts, is,

我们发现使用弥散形式的哈密顿约束会更方便。这需要注意所考虑流形边界上各物理量的衰减行为，库查尔已经在传统变量框架下对此做了讨论 [9]，而使用阿西特卡新变量 (除了记号改变之外) 并没有为该讨论新增内容，因此本文不再赘述。细节可以查阅文献 [8]。分部积分后的最终结果为，

$$\widetilde{H}\left(\widetilde{N}\right) := \frac{1}{G}\int dx N'_{\text{new}}\sqrt{E^x}\left[K_\varphi^2 - \frac{\left[\left(E^x\right)'\right]^2}{4\left(E^\varphi\right)^2} + \left(1 - \frac{2GM}{\sqrt{E^x}}\right)\right]. \tag{9}$$

and one has an additional pair of canonical variables at spatial infinity given by the proper time there and the *ADM* mass. In the quantum case, where the singularity is removed, one may have slices with two asymptotic regions, one outside and one inside the horizon. In that case, there will be a pair of canonical variables associated to each of the asymptotic infinities.

此外，空间无穷远处存在一对额外的正则变量，由该处的固有时和 *ADM* 质量给出。在量子情形，奇点会被消除，因此可能存在具有两个渐近区域的切片，一个在视界外，一个在视界内。这种情况下，每个渐近无穷远都会对应一对正则变量。

Quantization: Kinematics

量子化: 运动学

Let us proceed to the quantization. We need to take into account the extra variables at infinity we mentioned in the last section. For them we will just consider a traditional quantization based on square integrable functions of the *ADM* mass M . For the other variables, we will proceed with a loop-like quantization. It is natural to consider one-dimensional spin networks, graphs consistent of edges adjoining vertices along the radial direction. The variable K_x is proportional to the connection A_x so one can associate a traditional holonomy along the edges. The variable K_φ is a scalar and therefore is naturally associated with vertices. So for a given graph g , we will consider a basis of states,

我们现在开始进行量子化。我们需要考虑上一节提到的无穷远额外变量。对这些变量，我们仅采用基于 *ADM* 质量 M 平方可积函数的传统量子化。对其余变量，我们采用圈量子化方案。很自然地，我们可以考虑一维自旋网络，即由沿径向连接顶点的边构成的图。变量 K_x 与联络 A_x 成正比，因此可以为边赋予传统和乐。变量 K_φ 是标量，因此自然对应顶点。因此对给定图 g ，我们考虑如下态基，

$$|\vec{\mu},\vec{k}\rangle = \quad \overset{\cdots}{\underset{\mu_{j-1}}{\bullet}} \overset{k_j}{\underset{\mu_j}{\bullet}} \overset{k_{j+1}}{\underset{\mu_{j+1}}{\bullet}} \overset{\cdots}{} \quad ,$$

that can be translated into the connection representation as,

它可以转换为联络表示形式，即

$$T_{g,\vec{k},\vec{\mu}}\left(K_x, K_\varphi\right) = \prod_{e_j\in g}\exp\left(ik_j\int_{e_j} dx K_x\left(x\right)\right)\prod_{v_j\in g}\exp\left(i\mu_j K_\varphi\left(v_j\right)\right). \tag{10}$$

The labels k_j are integers and correspond to the ”color” of the edges e_j of the spin network associated with the graph g . The labels μ_j are real. So the kinematical Hilbert space we choose will be given by the direct product of the square integrable functions of the ADM mass M with the Hilbert space of square summable

functions corresponding to the holonomies of K_x times the Hilbert space of square integrable functions of the Bohr compactification [10] of the K_φ 's. This comes naturally endowed with an Ashtekar-Lewandowski [11] like inner product,

标签 k_j 为整数，对应与图 g 关联的自旋网络边 e_j 的“颜色”。标签 μ_j 是实数。因此我们选取的运动学希尔伯特空间可表示为:ADM 质量 M 的平方可积函数空间，乘以 K_x 和乐对应的平方可和函数希尔伯特空间，再乘以 K_φ 玻紧化 [10] 的平方可积函数希尔伯特空间的直积。该空间自然配备了 Ashtekar-Lewandowski[11] 型内积，

$$\left\langle \vec{k},\vec{\mu},M \mid \vec{k}',\vec{\mu}',M' \right\rangle = \delta_{\vec{k},\vec{k}'}\delta_{\vec{\mu},\vec{\mu}'}\delta\left(M-M'\right). \tag{11}$$

On the kinematical Hilbert space, the operator associated with the ADM mass acts multiplicatively, and the action of the triads is also straightforward, they also act multiplicatively,

在运动学希尔伯特空间上，与 ADM 质量关联的算子是乘法算子，三元基的作用也很直接，它们同样是乘法算子，

$$\widehat{M}\left|g,\vec{k},\vec{\mu},M\right\rangle = M\left|g,\vec{k},\vec{\mu},M\right\rangle, \tag{12}$$

$$\widehat{E}^x\left(x\right)\left|g,\vec{k},\vec{\mu},M\right\rangle = \ell_{\mathrm{Pl}}^2 k_j\left(x\right)\left|g,\vec{k},\vec{\mu},M\right\rangle, \tag{13}$$

$$\widehat{E}^\varphi\left(x\right)\left|g,\vec{k},\vec{\mu},M\right\rangle = \ell_{\mathrm{Pl}}^2 \sum_{v_j\in g}\delta\left(x-x_j\right)\mu_j\left|g,\vec{k},\vec{\mu},M\right\rangle, \tag{14}$$

where $k_j\left(x\right)$ is the valence of the edge that includes the point x . If it coincides with a vertex, we take the edge to the right. We denote the position of the vertex v_j as $x\left(v_j\right)$. We see that $\widehat{E}^\varphi\left(x\right)$ on this basis of states acts as a distribution due to the fact that classically it is a scalar density. We will concentrate on states based on a single graph, but superpositions with different graphs can also be considered, it just leads to more complex expressions. Superpositions were found to be relevant in the context of the fermion doubling problem [12].

其中 $k_j\left(x\right)$ 是包含点 x 的边的价。如果点恰好落在顶点上，我们取该顶点右侧的边。我们将顶点 v_j 的位置记为 $x\left(v_j\right)$。可以看到，$\widehat{E}^\varphi\left(x\right)$ 在该态基上作用为分布，这是因为经典层面上它是一个标量密度。我们这里集中讨论单图上的态，但也可以考虑不同图的叠加，只会得到更复杂的表达式。已有研究表明叠加在费米子加倍问题的背景下是相关的 [12]。

Concerning $K_\varphi\left(x\right)$, the only connection component that is present in the scalar constraint, the representation adopted for it will be in terms of point holonomies of length ρ , whose operators are,

关于标量约束中仅存的联络分量 $K_\varphi\left(x\right)$，我们对它采用点和乐表示，点和乐的长度为 ρ，其算子形式为，

$$N^\varphi_{\pm n\rho}\left(x\right)\left|g,\vec{k},\vec{\mu},M\right\rangle = \left|g,\vec{k},\vec{\mu}'_{\pm n\rho},M\right\rangle,\ n\in\mathbb{N}, \tag{15}$$

where the new vector $\vec{\mu}'_{\pm n\rho}$ either has just the same components than $\vec{\mu}$ up to $\mu_j \to \mu_j \pm n\rho$ if x coincides with a vertex of the graph located at x_j , or $\vec{\mu}'_{\pm n\rho}$ will be $\vec{\mu}$ with a new component $\{\ldots, \mu_j, \pm n\rho, \mu_{j+1}, \ldots\}$ with $x_j < x < x_{j+1}$.

其中若 x 与位于 x_j 的图顶点重合，新矢量 $\vec{\mu}'_{\pm n\rho}$ 的分量与 $\vec{\mu}$ 到 $\mu_j \to \mu_j \pm n\rho$ 的分量完全相同；否则，$\vec{\mu}'_{\pm n\rho}$ 等于 $\vec{\mu}$ 新增一个分量 $\{\ldots, \mu_j, \pm n\rho, \mu_{j+1}, \ldots\}$ (满足 $x_j < x < x_{j+1}$) 后的矢量。

One can also construct other geometrical operators of physical interest, at the kinematical level, like the total volume operator, given by

在运动学层面，我们还可以构造其他有物理意义的几何算子，例如总体积算子，其形式为

$$\widehat{\mathcal{V}} \left| g, \vec{k}, \vec{\mu}, M \right\rangle = 4\pi \ell_{\mathrm{Pl}}^3 \sum_{v_j \in g} \mu_j \sqrt{k_j} \left| g, \vec{k}, \vec{\mu}, M \right\rangle. \tag{16}$$

Dynamics: μ_0 Style Quantization

动力学: μ_0 样式量子化

To proceed to quantize the Hamiltonian constraint, we draw on the experience in loop quantum cosmology. The action of the basic kinematical operators can be viewed as involving an "LQC at each vertex" of the one-dimensional spin network. Just like in that case, the operator associated with K_φ is not a well-defined quantity, and one needs to "polymerize" the expressions involving it, in particular the Hamiltonian constraint, by doing the substitution $K_\varphi \to \sin\left(\rho K_\varphi\right)/\rho$. Here ρ is a fixed parameter that would correspond to the μ_0 of LQC, and it is assumed to be very small (zero in the classical limit). To promote the Hamiltonian constraint to an operator, it is convenient to rescale it, to take a square root (this simplifies finding solutions) and choose a factor ordering,

为了对哈密顿约束进行量子化，我们借鉴圈量子宇宙学中的经验。基本运动学算符的作用可以看作是在一维自旋网络的“每个顶点处都包含一个 LQC”。和圈量子宇宙学的情况一样，与 K_φ 关联的算符不是良定义的量，因此需要对包含它的表达式 (尤其是哈密顿约束) 进行“聚合”处理，通过代入替换 $K_\varphi \to \sin\left(\rho K_\varphi\right)/\rho$ 实现。此处 ρ 是一个固定参数，对应 LQC 的 μ_0 ，一般假定它很小 (经典极限下为零)。为了将哈密顿约束提升为算符，方便的做法是对其重新标度、开平方 (这会简化解的寻找过程) 并选择因子序，

$$\widehat{H}(N) = \int dx N(x) \left(2 \left\{ \sqrt{\sqrt{\widehat{E}^x} \left(1 + \sin^2\left(\rho \widehat{K}_\varphi\right)/\rho^2\right) - 2G\widehat{M}} \right\} \widehat{E}^\varphi - \sqrt[4]{\widehat{E}^x} \left(\widehat{E}^x\right)' \right). \tag{17}$$

The expression is readily promoted to an operator acting on the kinematical Hilbert space. We start with the action on spin network functions, introducing $y_j = K_\varphi\left(x_j\right)$,

该表达式可以直接提升为作用在运动学希尔伯特空间上的算符。我们从它对自旋网络函数的作用开始讨论，引入 $y_j = K_\varphi\left(x_j\right)$,

$$\widehat{H}(N)\, T_{g,\vec{k},\vec{\mu}}(K_x,\vec{y}) = \sum_{v_j\in g} N(v_j)\left(k_j \ell^2_{\text{Planck}}\right)^{\frac{1}{4}}$$

$$\left[\widehat{\sum}_j - \left(k_j - k_{j-1}\right)\ell^2_{\text{Planck}}\right] T_{g,\vec{k},\vec{\mu}}(K_x,\vec{y}). \tag{18}$$

with,

其中，

$$\widehat{\sum}_j = 2\sqrt{1+\frac{\sin^2(\rho y_j)}{\rho^2} - \frac{2G\widehat{M}}{\sqrt{k_j \ell^2_{\text{Planck}}}}}\,\ell^2_{\text{Planck}}\left(-i\partial_{y_j}\right) \tag{19}$$

Notice that the action of the Hamiltonian constraint keeps invariant the valences k_j . This allows one to restrict its action only on states associated with nondegenerate triads, that is, with non-vanishing k_j . This immediately implies, as we shall see in detail later on, the elimination of the singularities associated with degenerate triads and in particular it will eliminate the singularity inside black holes if one is to have the metric be a self-adjoint operator, as we will see in section "The Metric as a Dirac Observable."

注意哈密顿约束的作用保持价 k_j 不变。这使得我们可以将它的作用仅限制在与非退化三标架关联的态上，即具有非零 k_j 的态。正如我们之后会详细看到的，这直接意味着消除了与退化三标架关联的奇点，具体来说，如果我们将度规视为自伴算符，它就会消除黑洞内部的奇点，我们会在“作为狄拉克可观测量的度规”一节讨论这一点。

To proceed to find solutions of the Hamiltonian constraint, we try a solution of the type,

为了寻找哈密顿约束的解，我们尝试如下形式的解:

$$\Psi\left(K_\varphi, K_x, g, \vec{k}, M\right) = \sum_{v\in g}\sum_{\mu(v)} T_{g,\vec{k},\vec{\mu}}(K_x,K_\varphi)\,\Psi(\mu(v),M). \tag{20}$$

where, given (13) and (17), we will assume the integers k_i satisfy $k_1 < k_2 < \ldots < k_v$ with i going from 1 to V in order to avoid unnecessary redundancies in the description. From now on, we can omit the g dependence since we only include vertices where k_j changes, and therefore all information about the graph is included in the k_j ' s. The information about the k_j ' s can be codified in $\vec{k}$, and we will seek solutions with a given $\vec{k}$. It would be straightforward, though more complicated, to consider superpositions with different k_j ' s, so we will omit them here, but one would expect that generic states would involve them. It turns out that the Hamiltonian constraint can be solved, with the solution given by,

其中，结合式 (13) 和 (17)，我们假定整数 k_i 满足 $k_1 < k_2 < \ldots < k_v$ ，且 i 的取值范围为 1 到 V ，以避免描述中不必要的冗余。从现在开始，我们可以省略对 g 的依赖，因为我们仅包含 k_j 发生变化的顶点，因此图的所有信息都已经包含在 k_j 中。k_j 的信息可以编码在 $\vec{k}$ 中，我们将寻找给定 $\vec{k}$ 下的解。考虑不同 k_j 的叠加虽然更复杂，但操作起来很直接，因此我们在此省略，但一般认为普通态都会包含这类叠加。事实证明哈密顿约束是可解的，解由下式给出:

$$\Psi\left(K_\varphi, K_x, g, \vec{k}, M\right) = \exp\left(f\left(K_\varphi, g, \vec{k}, M\right)\right)\Pi_{e_j\in g}\exp\left(ik_j\int_{e_j} K_x(x)\,dx\right),$$

(21)

with the quantities

其中各量为

$$f = \sum_{v_j \in g} -\frac{i}{2}\Delta K_j m_j F\left(\sin\left(\rho K_\varphi\left(x_j\right), i m_j\right)\right), \tag{22}$$

and,

且,

$$\Delta K_j = k_j - k_{j-1}, \tag{23}$$

$$m_j = \left[\rho\sqrt{1 - 2GM/\sqrt{k_j}\ell_{\text{ Planck}}}\right]^{-1}, \tag{24}$$

$$F(\phi, m) = \int_0^{\phi}\left(1 - m^2\sin^2 t\right)^{-1/2} dt, \tag{25}$$

with the latter the Jacobi elliptic function of the first kind. These solutions to the constraint are well defined for both the exterior $\left(m_j^2 > 0\right)$ and the interior $\left(m_j^2 < 0\right)$ of the black hole. In particular, they belong to the kinematical Hilbert space in the sense that they have finite norm with respect to the inner product (11). See [4] for details. To complete the construction of physical states, one needs to group average these solutions so that the resulting averaged states are invariant under the transformations generated by the diffeomorphism constraint. This leads to states that are superpositions of spin networks with vertices along all the possible positions along the radial line. The order of the vertices has to be preserved. We will later see that this preservation leads to the appearance of new observables in the quantum theory. One is therefore left with elements of the physical space of states that are well-defined functions of K_x, K_φ labeled by the $\vec{k}$ and M , we will denote them as $|\vec{k}, M\rangle$, with inner product $\left\langle \vec{k}, M \mid \vec{k}', M' \right\rangle = \delta_{\vec{k},\vec{k}'}\delta\left(M - M'\right)$.

后者是第一类雅可比椭圆函数。这些约束解对黑洞外部 $\left(m_j^2 > 0\right)$ 和内部 $\left(m_j^2 < 0\right)$ 都是良定义的。具体来说，它们属于运动学希尔伯特空间，即相对于内积 (11) 它们具有有限范数，细节参见文献 [4]。为了完成物理态的构造，需要对这些解做群平均，使得平均后的态在微分同胚约束生成的变换下保持不变。这最终得到的态是径向线上所有可能位置顶点的自旋网络叠加。顶点的顺序必须保留。我们之后会看到，这种顺序保留会给量子理论带来新的可观测量。最终我们得到物理态空间中的元素，它们是 K_x, K_φ 的良定义函数，由 $\vec{k}$ 和 M 标记，我们将其记为 $|\vec{k}, M\rangle$ ，其内积为 $\left\langle \vec{k}, M \mid \vec{k}', M' \right\rangle = \delta_{\vec{k},\vec{k}'}\delta\left(M - M'\right)$ 。

Parameterized Dirac Observables

参数化狄拉克可观测量

Physical observables are operators that leave invariant the physical Hilbert space. We will use the technique known as parameterized Dirac observables (or evolving constants of the motion) to construct them. We

briefly review it. A parameterized Dirac observable has vanishing Poisson bracket with the constraints and depends on parameters (or in the case of field theories, functional parameters). They are used to describe the evolution, and more generally, gauge-dependent quantities in terms of Dirac observables and parameters in totally constrained systems.

物理可观测量是在物理希尔伯特空间上保持不变的算符。我们将采用名为参数化狄拉克可观测量 (也称为运动演化常数) 的方法来构造这类可观测量，在此做简要概述。参数化狄拉克可观测量与约束的泊松括号为零，且依赖于参数 (场论情形下为泛函参数)。在全约束系统中，它们被用来描述演化，更一般地说，可通过狄拉克可观测量和参数描述规范依赖量。

A simple example is given by the well-known parameterized free particle in one dimension. The canonical variables are p_0, q^0 and p, q . Where q^0 is Newtonian time and p_0 its canonical momentum. The constraint is $\phi = p_0 + p^2/(2m)$, and examples of independent Dirac observables are p and $x = q - pq^0/m$. A parameterized Dirac observable is $Q(t) = x + pt/m$ and it satisfies $\{\phi, Q(t)\} = 0$. One also has that $Q(t)|_{t=q^0} = q$ and $Q(t)|_{t=q^0+\Delta t} = q + p\Delta t/m$. Hence, the parametrized Dirac observable $Q(t)$ describes the position of the free particle (In a quantum theory, there is the question of the meaning of a classical parameter like t . This has led to a rich discussion of the role of real clocks in quantum theory that is beyond the scope of this review [13]). This is also the case in the quantum theory where the parametrized Dirac observables can be promoted to operators in the physical space of states that are annihilated by the constraints. These parametrized observables coincide with the natural ones in a Heisenberg picture, and moreover, comparison of the latter with a Schrödinger one in [15] shows explicitly the equivalence between the two pictures (for the relativistic particle).

一维已知的参数化自由粒子就是一个简单例子。正则变量为 p_0, q^0 和 p, q，其中 q^0 是牛顿时间，p_0 是其正则动量。约束为 $\phi = p_0 + p^2/(2m)$，独立狄拉克可观测量的例子为 p 和 $x = q - pq^0/m$。参数化狄拉克可观测量为 $Q(t) = x + pt/m$，满足 $\{\phi, Q(t)\} = 0$，同时还满足 $Q(t)|_{t=q^0} = q$ 和 $Q(t)|_{t=q^0+\Delta t} = q + p\Delta t/m$。因此参数化狄拉克可观测量 $Q(t)$ 描述了自由粒子的位置 (在量子理论中，像 t 这样的经典参数的物理含义存在争议，由此引发了关于真实时钟在量子理论中作用的大量讨论，这超出了本综述的范围 [13])。量子理论中也是如此，参数化狄拉克可观测量可以提升为被约束湮灭的物理态空间上的算符。这些参数化可观测量与海森堡绘景下的自然可观测量一致，此外，文献 [15] 中将海森堡绘景与薛定谔绘景对比，明确证明了两种绘景 (对相对论粒子而言) 是等价的。

Just like we were able to use a parameterized Dirac observable to represent the position of the particle in the above example (which is NOT a Dirac observable), we will be able to use parameterized Dirac observables to represent quantities like any element of the kinematical space, which are not Dirac observables in general relativity. This point tends to generate confusion, but the above example should make it clear. A parameterized Dirac observable does not have a well-defined value until one chooses a phase space variable (in this case q_0) or phase space function and identifies it with a (time) parameter. Similarly, a metric component is not well defined until one picks a coordinate system. Picking a parameterization (remember that these are functional parameters in the case of general relativity) therefore corresponds to a choice of space-time coordinates or slicings of space-time.

正如我们在上述例子中可以用参数化狄拉克可观测量描述粒子位置 (而位置本身不是狄拉克可观测量)，在广义相对论中我们也可以用参数化狄拉克可观测量描述运动学空间中任意这类本身不是狄拉克可观测量的量。这一点经常引发混淆，但上述例子已经把它讲清楚了。在选定相空间变量 (本例中为 q_0) 或相空间函数并将其等同于 (时间) 参数之前，参数化狄拉克可观测量没有明确定义。这就好比选定坐标系之前，度规分量没有明确定义一样。因此选择参数化 (注意广义相对论中这些是泛函参数) 就对应于选择时空坐标或时空切片。

As we mentioned, the order of the vertices is unchanged by the group averaging procedure. This is associated with the existence of a parameterized quantum Dirac observable that does not have a classical counterpart. It is given by,

如前所述，群平均过程不会改变顶点的顺序。这对应着一个不存在经典对应物的参数化量子狄拉克可观测量，它由下式给出:

$$\widehat{O}(z)\left|\vec{k},M\right\rangle = \ell^2_{\text{Planck}}\, k_{\text{Int(Vz)}}\left|\vec{k},M\right\rangle \tag{26}$$

where Int means integer part, V is the number of vertices in the spin network (itself a Dirac observable without classical counterpart), and z is a real parameter in the interval $[0,1]$. What this observable does is, as one slides the parameter between 0 and 1, to pick the various values of the valences of the spin network. As seen from its action, this parameterized Dirac observable keeps invariant the physical Hilbert state, as one expects for a Dirac observable.

其中 Int 表示整数部分，V 是自旋网中的顶点数 (它本身就是一个没有经典对应物的狄拉克可观测量)，z 是区间 $[0,1]$ 内的实参数。当参数在 0 到 1 之间滑动时，这个可观测量会选取自旋网不同的价值。从它的作用可以看出，正如狄拉克可观测量应当满足的性质，这个参数化狄拉克可观测量保持物理希尔伯特态不变。

We would also like to observe that the triads can be represented by parameterized Dirac observables. For E^x we have that,

我们还要指出，标架可以由参数化狄拉克可观测量表示。对于 E^x ，我们有:

$$\widehat{E}^x(x)\left|\vec{k},M\right\rangle = \widehat{O}(z(x))\left|\vec{k},M\right\rangle, \tag{27}$$

where $z(x) : [0,x] \to [0,1]$, an arbitrary monotonic function that plays the role of the (functional) parameter. Different choices of function correspond to representing the triad in different spatial coordinates. An expression for E^φ can be obtained by solving the Hamiltonian constraint, as it appears algebraically in it.

其中 $z(x) : [0,x] \to [0,1]$ 是一个任意单调函数，充当 (泛函) 参数的角色。不同的函数选择对应于在不同空间坐标下表示三元组。我们可以通过求解哈密顿约束得到 E^φ 的表达式，因为它代数地出现在该约束中。

Let us start by the classical expression for the Hamiltonian density that appears integrated in (17) $\mathcal{H}(x)$, given by,

我们先从 (17) 中被积分的哈密顿密度的经典表达式开始 $\mathcal{H}(x)$，它由下式给出:

$$\mathcal{H}(x)=2E^{\varphi}(x)\sqrt{\sqrt{E^{x}(x)}\left(1+K_{\varphi}(x)^{2}\right)-2GM}-\sqrt[4]{E^{x}(x)}[E^{x}(x)]^{\prime} \tag{28}$$

and let us define

接下来我们定义

$$H_{r}(x)=\frac{\mathcal{H}(x)}{2\sqrt{\sqrt{E^{x}(x)}\left(1+K_{\varphi}(x)^{2}\right)-2GM}} \tag{29}$$

which makes it obvious that it has weakly vanishing Poisson bracket with the Hamiltonian constraint. Now taking into account (28), we can define the parametrized observable,

由此可以明显看出它与哈密顿约束的泊松括号弱为零。现在结合 (28) 式，我们可以定义参数化可观测量:

$$\mathcal{E}^{\varphi}(x)=H_{r}(x)+\frac{[\varepsilon^{x}(x)]^{\prime}}{2\sqrt{1+\kappa_{\varphi}(x)^{2}-\frac{2GM}{\sqrt{\varepsilon^{x}}(x)}}}, \tag{30}$$

and this is a parameterized Dirac observable dependent on two functional parameters $\kappa_{\varphi}(x)$ and $\varepsilon^{x}(x)$ respectively associated to K_{φ} and E^{x}. It satisfies

这是一个依赖于两个泛函参数的参数化狄拉克可观测量，$\kappa_{\varphi}(x)$ 和 $\varepsilon^{x}(x)$ 分别关联于 K_{φ} 和 E^{x}。它满足

$$\mathcal{E}^{\varphi}(x)\big|_{\substack{K_{\varphi}=\kappa_{\varphi}\\ E^{x}=\varepsilon^{x}}}=E^{\varphi}(x). \tag{31}$$

Taking into account that $\widehat{H}_{r}$ vanishes on the physical space, the polimerization of K_{φ} and using the new observables $\widehat{O}(z)$ that appear at the quantum level, we can promote this parameterized observable to an operator acting on the physical space of states given by,

考虑到 $\widehat{H}_{r}$ 在物理空间上为零，K_{φ} 的聚合，以及量子层面出现的新可观测量 $\widehat{O}(z)$，我们可以将这个参数化可观测量提升为作用在物理态空间上的算符，形式为:

$$\widehat{E^{\varphi}}(x)=\frac{\frac{\widehat{O}(z(x)+1/V)-\widehat{O}(z(x))}{x(z+1/V)-x(z)}}{2\sqrt{1+\sin^{2}\left(\rho\alpha_{\varphi}(x)\right)/\rho^{2}-2GM/\sqrt{\widehat{O}(z(x))}}}, \tag{32}$$

that is a well-defined operator on the physical Hilbert space $\mathcal{H}_{\text{phys}}$.$z(x)$ and $\alpha_{\varphi}(x)$ are the parameters, and $x(z)$ is the inverse of the monotonic function $z(x)$. The expression that appears in the numerator is the quantum version of $[E^{x}(x)]^{\prime}$ that was taken as a functional parameter $[\varepsilon^{x}(x)]^{\prime}$ in the classical theory. In fact, $\widehat{O}(z(x)+1/V)\left|\vec{k},M\right\rangle=\ell^{2}_{\text{Planck}}\,k_{\text{Int}(Vz(x)+1)}\left|\vec{k},M\right\rangle$ and therefore,

它是物理希尔伯特空间上一个定义良好的算符，其中 $\mathcal{H}_{\text{phys}}.z(x)$ 和 $\alpha_\varphi(x)$ 是参数，$x(z)$ 是单调函数 $z(x)$ 的反函数。分子中的表达式是经典理论中被取作泛函参数 $[\varepsilon^x(x)]'$ 的 $[E^x(x)]'$ 的量子版本。事实上，$\widehat{O}(z(x)+1/V)\left|\vec{k},M\right\rangle = \ell^2_{\text{Planck}}\, k_{\text{Int}(Vz(x)+1)}\left|\vec{k},M\right\rangle$，因此

$$[E^x(x)]'\left|\vec{k},M\right\rangle = \frac{\ell^2_{\text{Planck}}\left(k_{\text{Int}(Vz(x)+1)} - k_{\text{Int}(Vz(x))}\right)}{x(z+1/V)-x(z)}\left|\vec{k},M\right\rangle. \tag{33}$$

A similar technique can be applied for the remaining kinematical variable $K_x(x)$ that can be promoted to a parameterized Dirac observable. We start with the classical phase space function $\mathcal{D}(x) = \left\{E^\varphi(x)\left[K_\varphi(x)\right]' - [E^x(x)]'K_x(x)\right\}$ obtained from the classical diffeomorphism constraint. Then, it is easy to verify that,

类似的方法也可应用于其余运动学变量 $K_x(x)$，它同样可以被提升为参数化狄拉克可观测量。我们从经典微分同胚约束得到的经典相空间函数 $\mathcal{D}(x) = \left\{E^\varphi(x)\left[K_\varphi(x)\right]' - [E^x(x)]'K_x(x)\right\}$ 出发，很容易可以验证:

$$\mathcal{K}_x(x) = -\frac{\mathcal{D}(x)}{E^x(x)'} + \frac{E^\varphi(x)\kappa_\varphi(x)'}{\varepsilon^x(x)'}, \tag{34}$$

satisfies $\mathcal{K}_x(x)\big|_{\substack{E^x=\varepsilon(x)^x\\ K_\varphi=\kappa_\varphi(x)}} = K_x(x)$, as it is required for a parameterized observable. As in the case of E^φ, upon quantization one has to take into account that $\widehat{E}^x(x) = \widehat{O}(z(x))$ and K_φ must be polymerized, which implies that $\kappa_\varphi(x) = \sin\left(\rho\alpha_\varphi(x)\right)/\rho$. Thus, the quantum parameterized observable is

它满足 $\mathcal{K}_x(x)\big|_{\substack{E^x=\varepsilon(x)^x\\ K_\varphi=\kappa_\varphi(x)}} = K_x(x)$，这正是参数化可观测量所要求的条件。和 E^φ 的情况一样，量子化过程中必须考虑到 $\widehat{E}^x(x) = \widehat{O}(z(x))$ 和 K_φ 需要聚合化，这意味着 $\kappa_\varphi(x) = \sin\left(\rho\alpha_\varphi(x)\right)/\rho$。因此，量子参数化可观测量为

$$\widehat{\mathcal{K}}_x(x) = \frac{\widehat{\mathcal{E}}^\varphi(x)\cos\left(\rho\alpha_\varphi(x)\right)\alpha'_\varphi(x)}{\frac{\widehat{O}(z(x)+1/V)-\widehat{O}(z(x))}{x(z+1/V)-x(z)}} \tag{35}$$

As it happened in the example of the free particle, one ends up having a system where all the kinematical variables are parameterized Dirac observables or pure parameters.

和自由粒子例子中的结果一致，最终得到的系统中所有运动学变量要么是参数化 Dirac 可观测量，要么是纯参数。

The Metric as a Dirac Observable

度量作为狄拉克可观测量

Using these results, one can write parameterized Dirac observables representing the various components of the space-time metric. We start by noticing that, from a space-time point of view, the parameterized observables introduced in the previous section correspond to stationary choices where K_φ and E^x are functions

of x independent of t . One can define the classical metric components in any stationary gauge by imposing the gauge fixing conditions $\Phi_1 = E^x(x) - \varepsilon^x(x)$ and $\Phi_2 = K_\varphi(x) - \kappa_\varphi(x)$, where $\varepsilon^x(x)$ and $\kappa_\varphi(x)$ are arbitrary functions that represent the choice of coordinates for stationary space-times. In many cases, the gauge functions might depend on the canonical variables and M as well. This is the case, for instance, of the well-known Eddington-Finkelstein coordinates (see the appendix of [14] for details). We additionally require that the resulting space-times be asymptotically flat. This restricts $\varepsilon^x(x) = x^2 + \mathcal{O}\left(x^{-1}\right)$ and $\kappa_\varphi(x) = \mathcal{O}\left(x^{-1}\right)$ in the limit $x \to \infty$. These conditions allow us to determine

利用这些结果，我们可以写出表示时空度量各分量的参数化狄拉克可观测量。我们首先注意到，从时空角度来看，上一节引入的参数化可观测量对应于定态选择，其中 K_φ 和 E^x 是 x 的函数，与 t 无关。我们可以通过施加规范固定条件 $\Phi_1 = E^x(x) - \varepsilon^x(x)$ 和 $\Phi_2 = K_\varphi(x) - \kappa_\varphi(x)$ 在任意定态规范中定义经典度量分量，其中 $\varepsilon^x(x)$ 和 $\kappa_\varphi(x)$ 是任意函数，代表定态时空的坐标选择。在许多情况下，规范函数也可能依赖于正则变量和 M 。例如，著名的爱丁顿-芬克斯坦坐标就是这种情况 (细节见文献 [14] 的附录)。我们额外要求所得时空是渐近平直的，这在极限 $x \to \infty$ 下对 $\varepsilon^x(x) = x^2 + \mathcal{O}\left(x^{-1}\right)$ 和 $\kappa_\varphi(x) = \mathcal{O}\left(x^{-1}\right)$ 给出了限制。这些条件允许我们确定

$$N(x)^2 = 1 + {\kappa_\varphi}^2(x) - \frac{2GM}{\sqrt{\varepsilon^x(x)}},\ N^x(x) = 2\frac{\kappa_\varphi(x)\sqrt{\varepsilon^x(x)}}{[\varepsilon^x(x)]'}\sqrt{1 + {\kappa_\varphi}^2(x) - \frac{2GM}{\sqrt{\varepsilon^x(x)}}},$$

(36)

up to an irrelevant constant of integration for the lapse $N(x)$ that is fixed by the condition $N(x) = 1 + \mathcal{O}\left(x^{-1}\right)$ in the limit $x \to \infty$. The classical metric components for stationary coordinates are $g_{xx}(x) = \left(\mathcal{E}^\varphi(x)\right)^2/\varepsilon^x(x)$

直到平移 $N(x)$ 的一个无关积分常数，该常数由极限 $x \to \infty$ 下的条件 $N(x) = 1 + \mathcal{O}\left(x^{-1}\right)$ 固定。定态坐标下的经典度量分量为 $g_{xx}(x) = \left(\mathcal{E}^\varphi(x)\right)^2/\varepsilon^x(x)$

$$g_{tx}(x) = g_{xx}(x)N^x(x) = -\frac{[\varepsilon^x(x)]'\kappa_\varphi(x)}{2\sqrt{\varepsilon^x(x)}\sqrt{1 + \kappa_\varphi(x)^2 - \frac{2GM}{\sqrt{\varepsilon^x(x)}}}}, \tag{37}$$

and a similar expression for $g_{tt}(x)$. Notice the role played by $K_\varphi(x)$ in this expression: it determines the slicing. For instance, $K_\varphi(x) = 0$ leads to co-moving slicings with $g_{tx}(x) = 0$ like the ones that cover the exterior of black holes only. Non-vanishing $K_\varphi(x)$'s will be needed for horizon penetrating slicings like the Painlevé-Gullstrand and Eddington-Finkelstein ones.

且 $g_{tt}(x)$ 有类似表达式。注意 $K_\varphi(x)$ 在该表达式中发挥的作用: 它决定了切片方式。例如, $K_\varphi(x) = 0$ 会得到带有 $g_{tx}(x) = 0$ 的共动切片, 这类切片仅覆盖黑洞外部。对于能穿过视界的切片 (如潘勒韦-古尔斯兰德切片和爱丁顿-芬克斯坦切片)，需要非零的 $K_\varphi(x)$ 。

The above expression is straightforwardly promoted to an operator acting on the physical space of states by taking into account the new observables $\widehat{O}(z(x))$, the polimerization of the extrinsic curvature $\kappa_\varphi(x) = \frac{\sin(\rho\alpha_\varphi(x))}{\rho}$, and the observable $\widehat{M}$. General gauge fixings may require considering functions $\alpha_\varphi\left(x, \widehat{M}, \widehat{O}\right)$. For instance, the metric component $\hat{g}_{tx}(x)$ takes the form,

通过考虑新可观测量 $\widehat{O}(z(x))$ 、外曲率 $\kappa_{\varphi}(x)=\frac{\sin(\rho\alpha_{\varphi}(x))}{\rho}$ 的聚合以及可观测量 $\widehat{M}$ ，上述表达式可以直接推广为作用在物理态空间上的算符。一般规范固定可能需要考虑函数 $\alpha_{\varphi}\left(x,\widehat{M},\widehat{O}\right)$ 。例如，度量分量 $\hat{g}_{tx}(x)$ 形如

$$\hat{g}_{tx}(x)=\frac{\widehat{\mathcal{E}}^{\varphi}(x)\sin\left(\rho\alpha_{\varphi}(x)\right)}{2\rho\sqrt{\widehat{O}(z(x))}}. \tag{38}$$

The square root that appears in $\widehat{\mathcal{E}}^{\varphi}(x)$ -see Eq. (32)-leads to the following inequality, in order to get a self-adjoint operator (notice that there are no factor ordering issues), $1+\left(\frac{\sin(\rho\alpha_{\varphi}(x))}{\rho}\right)^{2}-\frac{2GM}{\sqrt{\widehat{O}(z(x))}}\geq 0$. The inequality is violated when the eigenvalues of $E^{x}(x)$ become small. The most favorable choice of parameters, from the point of view of keeping the expression positive at that point is $\alpha_{\varphi}(x=0)=\pi/(2\rho)$ (since $E^{x}(x)$ is monotonic, the worse case happens at $x=0$). Therefore, the condition for the square root that appears in the metric for it to be real and therefore the metric operator self-adjoint is, in terms of the eigenvalues of $\widehat{E}^{x}$, given by, $k_0>\left(\frac{2GM}{\ell_{\text{Planck}}\left(1+\frac{1}{\rho^2}\right)}\right)^{2}$. As a consequence, given the fact that we take ρ small, sufficiently small values of k_0 are excluded in order to have a self-adjoint metric operator and as a consequence the singularity is avoided. The region exterior to the horizon is covered for any choice of $\alpha_{\varphi}(x)$ since the last term in the first inequality is less or equal to 1 outside the horizon. Notice that there exist choices of the parameters that would make the metric singular. Those correspond to coordinate singularities, and loop quantum gravity correctly does not eliminate them (as in the classical theory, they amount to pathological choices of parametrized observables).

为得到自伴算符 (注意不存在因子排序问题)，$\widehat{\mathcal{E}}^{\varphi}(x)$ 中 (见式 (32)) 出现的平方根给出如下不等式 $1+\left(\frac{\sin(\rho\alpha_{\varphi}(x))}{\rho}\right)^{2}-\frac{2GM}{\sqrt{\widehat{O}(z(x))}}\geq 0$ 。当 $E^{x}(x)$ 的特征值变小时，该不等式不成立。从保证该点表达式为正的角度来看，最有利的参数选择是 $\alpha_{\varphi}(x=0)=\pi/(2\rho)$ (由于 $E^{x}(x)$ 是单调的，最坏情况出现在 $x=0$)。因此，用 $\widehat{E}^{x}$ 的特征值表示，度规中平方根为实、从而度规算符自伴的条件由 $k_0>\left(\frac{2GM}{\ell_{\text{Planck}}\left(1+\frac{1}{\rho^2}\right)}\right)^{2}$ 给出。由此，由于我们取 ρ 为小量，要得到自伴度规算符就必须排除足够小的 k_0 取值，奇点因此得以避免。对于任意 $\alpha_{\varphi}(x)$ 选择，视界外区域都被覆盖，因为第一个不等式中的最后一项在视界外小于等于 1。请注意，存在某些参数选择会使得度规奇异。这些对应坐标奇点，圈量子引力没有消除它们是正确的——就像经典理论中一样，这些奇异来源于参数化可观测量的不良选择。

As we mentioned, the action of the Hamiltonian constraint and all Dirac observables leave the values of $\vec{k}$ invariant, so it is consistent to consider values of the k_j 's bigger than k_0 . This implies that the singularity that appears inside black holes in general relativity can be eliminated. This will also be the case in the improved quantization we discuss in the next section, but details will be different.

正如我们提到的，哈密顿约束和所有狄拉克可观测量的作用都保持 $\vec{k}$ 的值不变，因此认为 k_j 的值大于 k_0 是自洽的。这意味着广义相对论中出现在黑洞内部的奇点可以被消除。这一结论在下一节我们讨论的改进量子化中也成立，只是细节会有所不同。

The analysis can be extended to the interval $[-x_{+},x_{+}]$ with a simple generalization of $O(z)$ to $z\in[-1,1]$. The expectation value of the determinant of the space-time metric can be explicitly calculated in any given gauge, and it goes through a maximum value and starts decreasing for negative values of x . One can view

this as a generalization of the Kruskal extension including a new region that is reached by tunneling through the singularity.

我们可以将分析拓展到区间 $[-x_+, x_+]$，只需将 $O(z)$ 简单推广为 $z \in [-1,1]$ 即可。在任意给定规范中都可以显式计算时空度规行列式的期望值: 当 x 取负值时，该期望值先达到最大值后开始下降。可以将这一过程看作克鲁斯卡延拓的推广: 穿过奇点隧穿后会进入一个新区域。

Clearly, not all quantum states will exhibit semi-classical behavior. To begin with, a condition for good semi-classical states is that the separation of the vertices of the spin network be small with respect to the relevant radius of curvature. That would require consecutive values of the k_j's that are close to each other. The quantization of the areas of the spheres of symmetry imposes a minimum bound on the separation of consecutive points on the spin networks. For instance, for a black hole of mass M, close to the horizon its curvature is proportional to $(GM)^{-2}$, while the minimal separation of two points on the spin networks will be proportional to $\ell_{\text{Planck}}{}^2/GM$ there. For large black holes compared to the Planck scale, that is very small number. This allows to consider spin networks with very small separations of their vertices. They will approximate a smooth geometry exceedingly well. As mentioned, one can also consider states that are superpositions of several spin networks as well. These states will improve the semi-classical behavior.

显然，并非所有量子态都具有半经典行为。首先，良好半经典态的条件是: 自旋网顶点的间距远小于相关曲率半径，这要求相邻 k_j 的取值彼此接近。对称球面的面积量子化对自旋网上相邻点的间距给出了下界。例如，对于质量为 M 的黑洞，视界附近的曲率正比于 $(GM)^{-2}$，而自旋网上两点的最小间距在该处正比于 $\ell_{\text{Planck}}{}^2/GM$。对于远大于普朗克尺度的大黑洞，这个数值非常小，因此我们可以得到顶点间距极小的自旋网，它能极好地近似光滑几何。如前所述，我们也可以考虑多个自旋网叠加得到的态，这类态的半经典行为会更好。

Dynamics: Improved Quantization

动力学: 改进量子化

Up to now, we have considered a fixed polymerization parameter ρ. This is a μ_0 style quantization in the terminology of loop quantum cosmology. A problem associated with it is that the curvature near the region where the singularity used to be in the classical theory, although finite, can have very large values, it goes as $G^2M^2/\ell^4_{\text{Planck}}$. The improved quantization aligns better with what has been observed in singularity elimination in loop quantum cosmology, where no trans-Planckian behavior is observed.

到目前为止，我们一直考虑聚合参数 ρ 固定。这在圈量子宇宙学的术语中属于 μ_0 型量子化。与之相关的一个问题是，经典理论中原奇点附近的曲率虽然有限，但取值可以非常大，其变化规律为 $G^2M^2/\ell^4_{\text{Planck}}$。改进量子化与圈量子宇宙学中消除奇点的观测结果更契合，在该框架中未观测到跨普朗克行为。

We have seen that the basic mathematical building blocks of our quantum theory are 1-dimensional oriented graphs. Here we still consider graphs such that each contains a collection of consecutive edges e_j, each one associated with a vertex v_j. The kinematical Hilbert space $\mathcal{H}^{\text{grav}}_{\text{kin}}$ of the theory is characterized by a basis of states $|\vec{k}, \vec{\mu}\rangle$. Here, $k_j \in \mathbb{Z}$ and $\mu_j \in \mathbb{R}$ are valences of edges e_j and vertices $\left| \right. v_j$, respectively. The

treatment is similar to what has been done above, but now the point holonomies $\widehat{\mathcal{N}}_{\rho_j} := \widehat{\exp}\left(i\rho_j K_\varphi\left(x_j\right)\right)$ of the connection K_φ defined on a vertex v_j act as follows:

我们已经知道，我们量子理论的基础数学构件是一维定向图。这里我们仍考虑这类图: 每个图包含一组连续边 e_j ，每条边对应一个顶点 v_j 。该理论的运动学希尔伯特空间 $\mathcal{H}_{\text{kin}}^{\text{grav}}$ 分别由一组态基 $\left|\vec{k},\vec{\mu}\right\rangle$. Here, $k_j \in \mathbb{Z}$ and $\mu_j \in \mathbb{R}$ are valences of edges e_j and vertices v_j 表征。处理方式与上文类似，但现在定义在顶点 v_j 处的联络 K_φ 的点和乐 $\widehat{\mathcal{N}}_{\rho_j} := \widehat{\exp}\left(i\rho_j K_\varphi\left(x_j\right)\right)$ 作用如下:

$$\widehat{N}_{\rho_j}\left|\mu_j\right\rangle = \left|\mu_j + \rho_j\right\rangle, \tag{39}$$

where ρ now depends on j .

其中 ρ 现在依赖于 j 。

An improved quantization for these types of models was first proposed by Chiou et al. [16]. The idea is very similar to the improved quantization of LQC [10]: one relates the polymerization parameter to the area gap,

这类模型的改进量子化最早由 Chiou 等人 [16] 提出。其思路与 LQC[10] 的改进量子化非常相似: 将聚合参数与面积间隙关联起来,

$$4\pi\ell_{\text{Pl}}^2 k_j \overline{\rho}_j^{-2} = \Delta \tag{40}$$

This can be viewed as associating the point holonomy of the K_φ with a plaquette enclosing an area Δ , the first non-zero eigenvalue of the area operator in loop quantum gravity, of the order of ℓ_{Planck}^2 . Here $\ell_{\text{Pl}}^2 k_j$ is the eigenvalue of the kinematical operator $\widehat{E}^x\left(x_j\right)$, defined in Eq. (13). Now, point holonomies (39) of

这可以理解为将 K_φ 的点和乐与一个围出面积 Δ 的小斑块关联起来，该面积是圈量子引力中面积算符第一个非零本征值，量级为 ℓ_{Planck}^2 。式 (13) 中定义了运动学算符 $\widehat{E}^x\left(x_j\right)$ ，此处 $\ell_{\text{Pl}}^2 k_j$ 是该算符的本征值。那么，式 (39) 中的点和乐

"length" $\overline{\rho}_j$ will produce a shift in a state $\left|\mu_j\right\rangle$, which depends on the spectrum of some kinematical operators. Concretely, $\left|\mu_j\right\rangle \to \left|\mu_j + \overline{\rho}_j\right\rangle$, and given the above relation,

“长度” $\overline{\rho}_j$ 会使态 $\left|\mu_j\right\rangle$ 产生平移，该平移依赖于某些运动学算符的谱。具体而言，$\left|\mu_j\right\rangle \to \left|\mu_j + \overline{\rho}_j\right\rangle$ ，结合上述关系可得

$$\overline{\rho}_j = \sqrt{\frac{\Delta}{4\pi\ell_{\text{Pl}}^2 k_j}}. \tag{41}$$

Therefore, it will be convenient to adopt a more appropriate state labeling $\left|v_j\right\rangle$ with $v_j = \sqrt{k_j}\mu_j/\lambda$, and $\lambda^2 = \Delta/4\pi\ell_{\text{Pl}}^2$. Point holonomies of the form $\widehat{\mathcal{N}}_{\overline{\rho}_j} := \widehat{\exp}\left(i\overline{\rho}_j K_\varphi\left(x_j\right)\right)$ again have a well-defined and simple action on this new (single-vertex) state basis of $\mathcal{H}_{\text{kin}}^{\text{grav}}$

因此，对 $\mathcal{H}^{\text{grav}}_{\text{kin}}$ 采用以 $|v_j\rangle$ 、$v_j = \sqrt{k_j}\mu_j/\lambda$ 和 $\lambda^2 = \Delta/4\pi\ell^2_{\text{Pl}}$ 标记的更合适的态标号会更方便。形式为 $\widehat{\mathcal{N}_{\bar{\rho}_j}} := \widehat{\exp}\left(i\bar{\rho}_j K_\varphi(x_j)\right)$ 的点和乐在这个新的 (单顶点) 态基上依然有定义良好的简单作用。

$$\widehat{\mathcal{N}_{\bar{\rho}_j}}\,|v_j\rangle = |v_j + 1\rangle\,. \tag{42}$$

The physical space of states annihilated by the constraints can be obtained through a procedure similar to the one we followed before. The main difference is that the polymerization adopted for the extrinsic curvature $K_\varphi(x)$ takes the form $\sin\left(\rho_j K_\varphi(x_j)\right)/\rho_j$. Using those techniques one can check that the physical space of states is identified by the same basis and has the same observables that in the previous approach. The main difference one has is the change of polymerization, and this has implications in the details of how the singularity is eliminated.

被约束零化的物理态空间可以通过与我们此前采用的类似流程得到。主要区别在于,对外曲率 $K_\varphi(x)$ 采用的聚合化形式为 $\sin\left(\rho_j K_\varphi(x_j)\right)/\rho_j$ 。使用这些方法可以验证，物理态空间的基与可观测量均和先前方法中的一致。唯一的核心差异就是聚合化的改变，这会在奇点消除的具体细节上产生影响。

Singularity Elimination and Space-Time Extensions

奇点消除与时空延拓

As we discussed in section "The Metric as a Dirac Observable," in order to have a self-adjoint operator for the metric as a parameterized Dirac observable, one needs to limit the range of k_j 's to a range larger than a minimum number k_0 . That minimum number is of order unity. This is due to the fact that the polymerization parameter ρ is small. This requires some explanation. In full loop quantum gravity, the polymerization parameter would be associated with the minimum area of a loop, given by the quantum of area of the theory. Therefore, compared to features of a semi-classical solution in the exterior of macroscopic black hole, it is a very small number. Here, since we are dealing with point holonomies, the polymerization parameter is dimensionless. So there is less clear guidance on its value. Yet, if we believe that we should be capturing features of the full theory, one necessarily has to conclude the parameter must be small. This is important because the condition of a minimum k_0 that is of order unity is a very sensible condition in the context of a discrete geometry. Having a "hole" in the manifold that is of the order of the point separation in its discrete geometry means that if one is considering a semi-classical solution such a hole would not be a distinct feature. This is important because it corresponds to the region where the singularity is present in the classical theory. Furthermore, in the case of the improved quantization, the polymerization parameter is a ratio of length scales (or more precisely, the square root of a ratio of areas), $\rho_j\sqrt{\Delta/k_j\ell^2_{Pl}}$. Therefore, a natural argument would be to limit k_j to ensure that the area $k_j\ell^2_{Pl}$ be bounded below by Δ (i.e., LQG gives a lower bound on allowed non-zero areas).

正如我们在“作为狄拉克可观测量的度量”一节中讨论的，要让度量作为参数化狄拉克可观测量得到自伴算子，需要将 k_j 的取值范围限制在大于最小值 k_0 的区间内。该最小值为一阶量级，这是因为聚合参数 ρ 很小，对此我们需要稍作解释。在完整的圈量子引力中，聚合参数与圈的最小面积相关，由该理论的面积量子给出。因此，对比宏观黑洞外部半经典解的特征，它是一个非常小的量。在本文研究中，由于我们处理的是点和乐，聚合参数是无量纲的，因此其取值没有明确的指引。但如果我们认为该研究应当捕捉完整理论的特征，就必然得出该参数必须很小的结论。这一点很重要，因为量级为一阶的最小值 k_0 的条件，在离散几何框架下是非常合理的。流形上存在一个大小与离散几何点间距相当的“空洞”，意味着在半经典解中，这个空洞不会成为显著特征。而这一区域恰好对应经典理论中奇点存在的区域，因此十分重要。此外，在改进量子化方案中，聚合参数是长度尺度的比值 (更准确地说，是面积比的平方根)，即 $\rho_j\sqrt{\Delta/k_j\ell_{Pl}^2}$。因此，一个自然的推导是限制 k_j，以保证面积 $k_j\ell_{Pl}^2$ 存在不小于 Δ 的下界 (即圈量子引力给出了允许的非零面积的下界)。

In what follows, in order to analyze the implications of the improved dynamics in the singularity resolution, we will work with spin networks with a finite but large number of vertices V . For simplicity, we restrict the study to spin networks whose values of k_j are associated with a lattice with equidistant spacing such that,

下文我们将分析改进动力学对奇点解决的影响，因此采用顶点数 V 有限但很大的自旋网络进行研究。为简化推导，我们将研究限制在满足以下条件的自旋网络: 其 k_j 值对应等距间距晶格，即

$$x_j = \delta x\,(|j| + j_0)\,, \tag{43}$$

where $j \in \mathbb{Z}$ and $j_0 \geq 1$ is an integer that will be specified below, and δx is the step of the lattice of the coordinate x that we choose to be $\delta x = \ell_{\rm Pl}$. This choice amounts to choosing the function $z\,(x) \in [-1, 1]$ as $z\,(x) = x/\,(V\delta x)$, such that $z\left(x_j\right) = \text{sign}\,(j)\,(|j| + j_0)\,/V$, and we choose the semi-classical basis elements $k_j = (|j| + j_0)^2$.

其中 $j \in \mathbb{Z}$ 和 $j_0 \geq 1$ 是后文中将指定的整数，δx 是坐标 x 对应晶格的步长，我们将其取为 $\delta x = \ell_{\rm Pl}$。该选择等价于将函数 $z\,(x) \in [-1, 1]$ 取为 $z\,(x) = x/\,(V\delta x)$，满足 $z\left(x_j\right) = \text{sign}\,(j)\,(|j| + j_0)\,/V$，同时我们选取半经典基元 $k_j = (|j| + j_0)^2$.

For instance, in this family of states, the triad E^x and its spatial derivative can be easily represented as physical parametrized observables as,

例如，在这一族态中，标架 E^x 及其空间导数可以很容易地表示为物理参数化可观测量，即

$$\widehat{E}^x\left(x_j\right)\left|\vec{k}, M\right\rangle = \widehat{O}\left(z\left(x_j\right)\right)\left|\vec{k}, M\right\rangle = \ell_{\rm Pl}^2 k_j\left|\vec{k}, M\right\rangle = x_j^2\left|\vec{k}, M\right\rangle. \tag{44}$$

$$\left[\widehat{E}^x\left(x_j\right)\right]'\left|\vec{k}, M\right\rangle = \frac{\left(x_j + \delta x\right)^2 - x_j^2}{\delta x^2}\left|\vec{k}, M\right\rangle = \text{sign}\,(j)\left(2x_j + \delta x\right)|\vec{k}, M\rangle. \tag{45}$$

We now consider the action of the parametrized Dirac observable $\widehat{\mathcal{E}^\varphi}$

我们现在考虑参数化狄拉克可观测量 $\widehat{\mathcal{E}^\varphi}$ 的作用

$$\left(\widehat{\mathcal{E}}^{\varphi}\left(x_j\right)\right)=\frac{\left[\widehat{E}^{x}\left(x_j\right)\right]'/2}{\sqrt{1+\frac{\sin^2\left(\overline{\rho}_j\alpha_{\varphi}(x_j)\right)}{\overline{\rho}_j^2}-\frac{2G\widehat{M}}{\sqrt{|\widehat{E}^{x}(x_j)|}}}}, \tag{46}$$

where $\alpha_{\varphi}\left(x_j\right)$ can depend on $\widehat{M}$ or $\widehat{O}\left(z\right)$. For instance, for Eddington-Finkelstein coordinates.

其中 $\alpha_{\varphi}\left(x_j\right)$ 可以依赖 $\widehat{M}$ 或 $\widehat{O}\left(z\right)$。例如，在爱丁顿-芬克斯坦坐标系中。

$$\frac{\sin^2\left(\overline{\rho}_j\alpha_{\varphi}\left(x_j\right)\right)}{\overline{\rho}_j^2}=\frac{\left(2G\widehat{M}\right)^2}{\widehat{O}\left(z\left(x_j\right)\right)}\frac{1}{1+\frac{2G\widehat{M}}{\sqrt{\widehat{O}(z(x_j))}}}. \tag{47}$$

In order for $\widehat{\mathcal{E}}^{\varphi}$ to be a well-defined self-adjoint operator we have the condition, in terms of eigenvalues,

为了使 $\widehat{\mathcal{E}}^{\varphi}$ 成为定义良好的自伴算子，我们用本征值给出如下条件，

$$1+\frac{\sin^2\left(\overline{\rho}_j\alpha_{\varphi}\left(x_j\right)\right)}{\overline{\rho}_j^2}-\frac{2GM}{\sqrt{E^{x}\left(x_j\right)}}>0,\ \forall x_j,M. \tag{48}$$

This implies a minimum eigenvalue of $\widehat{E}^{x}\left(x_j\right)$, $\ell_{\mathrm{Pl}}^2k_0$, and at this point, the curvature is maximum. Let us analyze this situation in some detail. It implies both $\sin\left(\overline{\rho}_j\alpha_{\varphi}\left(x_j\right)\right)=1$, and $\overline{\rho}_j$ given by (41). For a given mass M, the smallest area of the 2-spheres must be such that

这意味着 $\widehat{E}^{x}\left(x_j\right)$, $\ell_{\mathrm{Pl}}^2k_0$ 存在最小本征值，此时曲率达到最大值。我们来详细分析这一情况: 它同时满足由 (41) 给出的 $\sin\left(\overline{\rho}_j\alpha_{\varphi}\left(x_j\right)\right)=1$ 和 $\overline{\rho}_j$。对于给定质量 M，二维球面的最小面积必定满足

$$\left(1+\frac{4\pi\ell_{\mathrm{Pl}}^2k_0}{\Delta}\right)-\frac{2GM}{\sqrt{\ell_{\mathrm{Pl}}^2k_0}}>0. \tag{49}$$

Assuming that $k_0\gg1$, we get

假设 $k_0\gg1$，我们得到

$$k_0>\left(\frac{2GM\Delta}{4\pi\ell_{\mathrm{Pl}}^3}\right)^{2/3}=\tilde{k}_0. \tag{50}$$

Now, since $\Delta\simeq\ell_{\mathrm{Pl}}^2$, the limit $k_0\gg1$ implies $M\gg m_{\mathrm{Pl}}$. This would correspond to large black holes (compared to the Planck mass). Let us take into account the first integer k_0 that is larger than $\tilde{k}_0$. For states with $\tilde{k}_0\gg1$, the minimum value of the smallest 2-sphere is (This scaling with the mass is in agreement with the prescription proposed by Ashtekar, Olmedo and Singh [5].)

现在，由于 $\Delta\simeq\ell_{\mathrm{Pl}}^2$，极限 $k_0\gg1$ 推出 $M\gg m_{\mathrm{Pl}}$。这对应于 (和普朗克质量相比的) 大黑洞。我们取大于 $\tilde{k}_0$ 的第一个整数 k_0。对于满足 $\tilde{k}_0\gg1$ 的态，最小二维球面的最小值为 (这种随质量的标度关系与 Ashtekar、Olmedo 和 Singh 提出的方案一致 [5])

$$k_0 \simeq \tilde{k}_0 \propto M^{2/3}. \tag{51}$$

After polymerizing K_φ , we will represent its presence in the metric via a function $F\left(x_j\right) \in [-1,1]$,

聚合 K_φ 后，我们将通过函数 $F\left(x_j\right) \in [-1,1]$, 表示它在度规中的存在

$$\sin^2\left(\overline{\rho}_j \alpha_\varphi\left(x_j\right)\right) = \left[\widehat{F}\left(x_j\right)\right]^2 \tag{52}$$

and different choices of $F\left(x_j\right)$ correspond to different slices. The metric operator can be written as,

且 $F\left(x_j\right)$ 的不同选择对应不同的切片，度规算子可以写为:

$$\hat{g}_{tt}\left(x_j\right) = -\left(1 - \frac{\hat{r}_S}{\sqrt{\widehat{E}^x\left(x_j\right)}}\right), \tag{53}$$

$$\hat{g}_{tx}\left(x_j\right) = -\sqrt{\frac{\pi}{\Delta}} \frac{\left\{\left[\widehat{E^x\left(x_j\right)}\right]'\right\}\sqrt{\left[\widehat{F}\left(x_j\right)\right]^2}}{\sqrt{1 - \frac{\hat{r}_S}{\sqrt{\widehat{E}^x\left(x_j\right)}} + \frac{4\pi\widehat{E}^x\left(x_j\right)\left[\widehat{F}\left(x_j\right)\right]^2}{\Delta}}}, \tag{54}$$

$$\hat{g}_{xx}\left(x_j\right) = \frac{\left\{\left[\widehat{E^x\left(x_j\right)}\right]'\right\}^2}{4\widehat{E}^x\left(1 - \frac{\hat{r}_S}{\sqrt{\widehat{E}^x\left(x_j\right)}} + \frac{4\pi\widehat{E}^x\left(x_j\right)\left[\widehat{F}\left(x_j\right)\right]^2}{\Delta}\right)}, \tag{55}$$

$$\hat{g}_{\theta\theta}\left(x_j\right) = \widehat{E}^x\left(x_j\right),\ \hat{g}_{\phi\phi}\left(x_j\right) = \widehat{E}^x\left(x_j\right)\sin^2\theta, \tag{56}$$

with $\hat{r}_S = 2G\widehat{M}$. And in terms of this operator, we can obtain an effective metric assuming we are in a semi-classical situation as $g_{\mu\nu} = \left\langle \hat{g}_{\mu\nu} \right\rangle$. We can take the expectation value as we have the metric written as an operator acting on the physical space of states annihilated by the constraints. For the states considered, this is straightforward as they are eigenstates.

其中 $\hat{r}_S = 2G\widehat{M}$ 。用该算子，我们可以在半经典情形 $g_{\mu\nu} = \left\langle \hat{g}_{\mu\nu} \right\rangle$ 下得到有效度规。由于度规已被写为作用在被约束湮灭的物理态空间上的算子，我们可以直接取期望。对于所考虑的态，这很简单，因为它们都是本征态。

To compare with traditional classical results in terms of a metric geometry, we will make some additional assumptions. We will consider the leading quantum corrections when the dispersion of the mass can be neglected. We can then proceed to drop all hats in the above expression and call the result ${}^{(0)}g_{\mu\upsilon}\left(x_j\right)$. We also take, for convenience, a continuum limit where $x_j = \delta x\,|j| + x_0$ is replaced by $(|x| + x_0)$, with $x \in \mathbb{R}$. We keep terms $\delta x / x_j$ writing them as $\delta x / (|x| + x_0)$ at first order. This implies that the effective geometries "bounce" when they reach $x = 0$.

为了和传统经典度规几何的结果对比，我们补充一些假设。考虑质量弥散可以忽略时的领头量子修正，我们可以在上式中去掉所有帽子，将结果记为 ${}^{(0)}g_{\mu\nu}\left(x_j\right)$。为方便起见，我们还取连续极限，将 $x_j=\delta x\,|j|+x_0$ 替换为 $(|x|+x_0)$，其中 $x\in\mathbb{R}$。我们保留 $\delta x/x_j$ 项，在一阶将它们写为 $\delta x/\left(|x|+x_0\right)$。这意味着有效几何到达 $x=0$ 时会发生“反弹”。

Let us consider as example the Painlevé-Gullstrand coordinates [18]. They correspond to

我们以 Painlevé-Gullstrand 坐标为例 [18]，它对应

$$\widehat{F}\left(x_j\right)=\overline{\rho}_j\sqrt{\frac{\hat{r}_S}{\sqrt{\widehat{E}^x\left(x_j\right)}}}. \tag{57}$$

This choice is equivalent to a lapse operator $\widehat{N}\left(x_j\right)=\hat{I}$. Notice that the function $F_1(x)<1$ for all $x\neq 0$, while $F_1(x=0)=1$. This will allow to probe the high curvature region of the effective geometry. The metric can be written as,

该选择等价于移时算子 $\widehat{N}\left(x_j\right)=\hat{I}$。注意对所有 $x\neq 0$，函数 $F_1(x)<1$ 成立，而 $F_1(x=0)=1$。这允许我们探测有效几何的高曲率区域。度规可以写为:

$${}^{(0)}g_{tt}(x)=-\left(1-\frac{r_S}{|x|+x_0}\right), \tag{58}$$

$${}^{(0)}g_{tx}(x)=-\operatorname{sign}(x)\sqrt{\frac{r_S}{|x|+x_0}}\left(1+\frac{\delta x}{2\left(|x|+x_0\right)}\right), \tag{59}$$

$${}^{(0)}g_{xx}(x)=\left(1+\frac{\delta x}{2\left(|x|+x_0\right)}\right)^2,\ {}^{(0)}g_{\theta\theta}(x)=\left(|x|+x_0\right)^2, \tag{60}$$

$${}^{(0)}g_{\phi\phi}(x)=\left(|x|+x_0\right)^2\sin^2\theta. \tag{61}$$

For large x, the metric approximates extremely well the Schwarzschild solution in Painlevé-Gullstrand coordinates. The curvature reaches its maximum when $F(x)=1$, at $x=0$. It is convenient to go to a diagonal gauge,

对于大 x，该度规对 Painlevé-Gullstrand 坐标下的史瓦西解有极好的近似。当 $F(x)=1$ 时，曲率达到最大值，此时为 $x=0$。转为对角规范会更方便，

$${}^{(0)}g_{xx}(x)\to{}^{(0)}\tilde{g}_{xx}(x)=\frac{\left(1+\frac{\delta x}{2(|x|+x_0)}\right)^2}{\left(1-\frac{r_s}{|x|+x_0}\right)},\ {}^{(0)}g_{tx}(x)\to{}^{(0)}\tilde{g}_{tx}(x)=0, \tag{62}$$

while all other components remain as

而所有其他分量保持为

$${}^{(0)}g_{tt}(x)\to{}^{(0)}\tilde{g}_{tt}(x)=-\left(1-\frac{r_S}{|x|+x_0}\right), \tag{63}$$

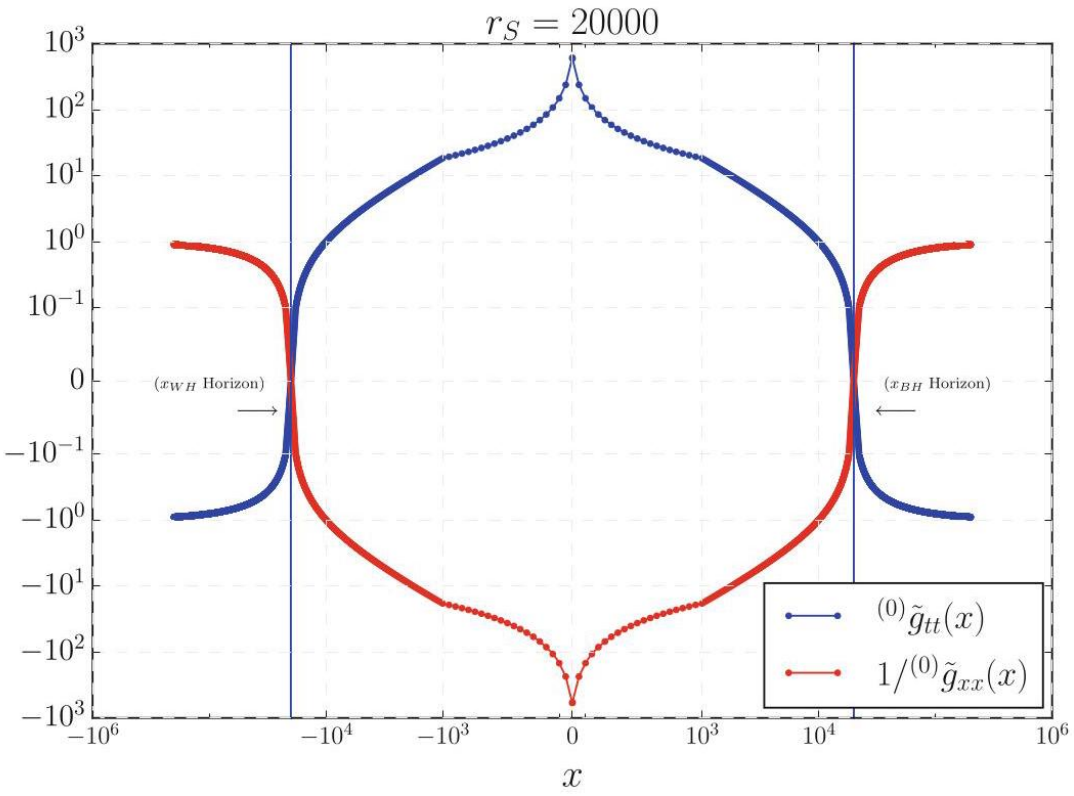

Fig. 1 The tt component of the metric and the inverse of xx for the metric in diagonal coordinates. When the first vanishes, horizons arise. Notice that in the region between the two horizons, the discreteness is more manifest and is represented in the separation of the dots (the plot does not show all the points in the lattice but only one out of 50). (Reproduced from reference [18])

图 1 对角坐标下度量的 tt 分量与 xx 的倒数。当第一个分量归零时，就会产生视界。请注意，在两个视界之间的区域，离散性更加明显，体现为点与点之间的间隔 (该图仅显示格点中每 50 个点里的 1 个，未展示全部格点)。(转载自参考文献 [18])

$$^{(0)}g_{\theta\theta}(x) \to {}^{(0)}\tilde{g}_{\theta\theta}(x) = (|x| + x_0)^2,\ {}^{(0)}g_{\varphi\varphi}(x) \to {}^{(0)}\tilde{g}_{\varphi\varphi}(x) = (|x| + x_0)^2 \sin\theta\ . \quad (64)$$

Figure 1 shows the values of the tt and inverse xx components of the metric, where one sees the emergence of two regions where one has a horizon, one for positive values of x , and one for negative ones [18]. This would correspond to a Penrose diagram as that of Fig. 2, which is reminiscent of Reissner-Nordstrom, but singularity-free.

图 1 展示了度量的 tt 分量与 xx 分量的倒数的取值，从中可以看出存在两个产生视界的区域，一个对应 x 取正值，另一个对应 x 取负值 [18]，对应的彭罗斯图如图 2 所示，该图类似赖斯纳-诺德斯特姆图，但无奇点。

In terms of the semi-classical metric, we can compute an effective stress tensor by computing the Einstein tensor, $T_{\mu\nu} := \frac{1}{8\pi G} G_{\mu\nu}$, and for it define the effective densities and pressures by taking into account that the Killing vector $X^\mu = (\partial_t)^\mu$ of the metric (62) will be time-like or space-like as one traverses the horizons of the black hole of the Penrose diagram shown in Fig. 2. In summary,

根据半经典度量，我们可以通过计算爱因斯坦张量 $T_{\mu\nu} := \frac{1}{8\pi G}G_{\mu\nu}$ 得到有效应力张量，再对其定义有效密度与压强，其中需要注意的是，对于图 2 所示彭罗斯图的黑洞，当穿过视界时，式 (62) 中度量的基林矢量 $X^\mu = (\partial_t)^\mu$ 会变为类时或类空。综上，

$$\rho^{ext} := -T_{\mu\upsilon}\frac{X^\mu X^\upsilon}{X^\rho X_\rho}, \tag{65}$$

$$p_x^{ext} := T_{\mu\upsilon}\frac{r^\mu r^\upsilon}{r^\rho r_\rho}, \tag{66}$$

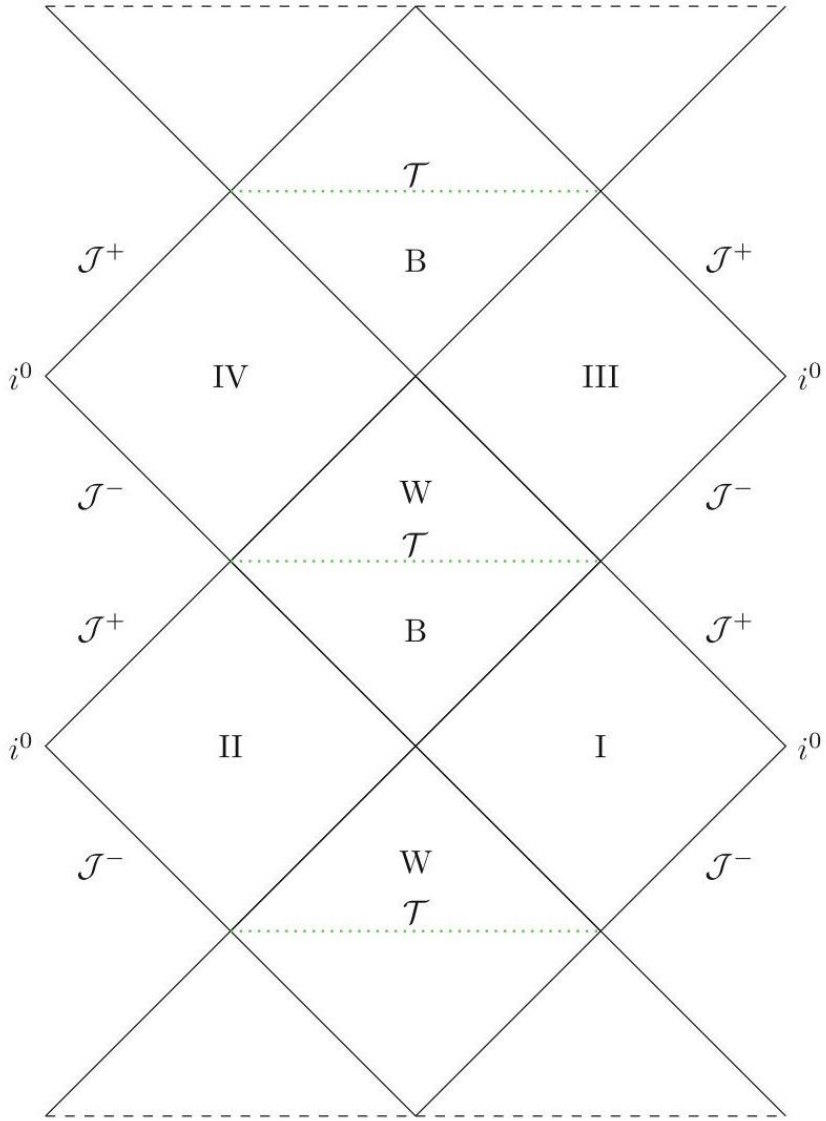

Fig. 2 Penrose diagram of the effective geometry discussed in the text. B and W denote a black hole and white hole, respectively. The horizontal lines separating them correspond to regions of high curvature. Regions I, II, III, IV approximate very well the Schwarzschild exterior. (Reproduced from reference [18])

图 2 正文中讨论的有效几何的彭罗斯图。B 和 W 分别表示黑洞和白洞。分隔二者的水平线对应高曲率区域。区域 I、II、III、IV 可以非常好地近似史瓦西外部区域。(转载自参考文献 [18])

and

且

$$p_{\|}^{ext} := T_{\mu\upsilon}\frac{\theta^{\mu}\theta^{\upsilon}}{\theta^{\rho}\theta_{\rho}}, \tag{67}$$

and for the interior,

对于内部，

$$\rho^{\,\mathrm{int}} := -T_{\mu\upsilon}\frac{r^{\mu}r^{\upsilon}}{r^{\rho}r_{\rho}}, \tag{68}$$

$$p_{x}^{\mathrm{int}} := T_{\mu\upsilon}\frac{X^{\mu}X^{\upsilon}}{X^{\rho}X_{\rho}}, \tag{69}$$

and notice that $p_{\|}^{\mathrm{int}} = p_{\|}^{\mathrm{ext}}$ as θ^{μ} remains space-like.

注意到 $p_{\|}^{\mathrm{int}} = p_{\|}^{\mathrm{ext}}$ 与 θ^{μ} 仍保持类空。

Figure 3 shows a plot of these components. As can be seen, negative values develop in the region where the singularity is replaced by a bounce. Although there are no violations of the strong energy condition as the energy density $\rho^{\,\mathrm{int}}$ is always positive, there is violation of the dominant energy condition. One can therefore see this effective semi-classical violation as explaining how it circumvents the singularity theorems in the interior of the black hole in the semi-classical picture.

图 3 绘制了这些分量。可以看出，在奇点被反弹替代的区域出现了负值。虽然由于能量密度 $\rho^{\,\mathrm{int}}$ 始终为正，强能量条件未被违反，但主能量条件确实被违反了。因此，我们可以将这种有效半经典层面的违反，看作半经典图像中对黑洞内部如何绕过奇点定理的解释。

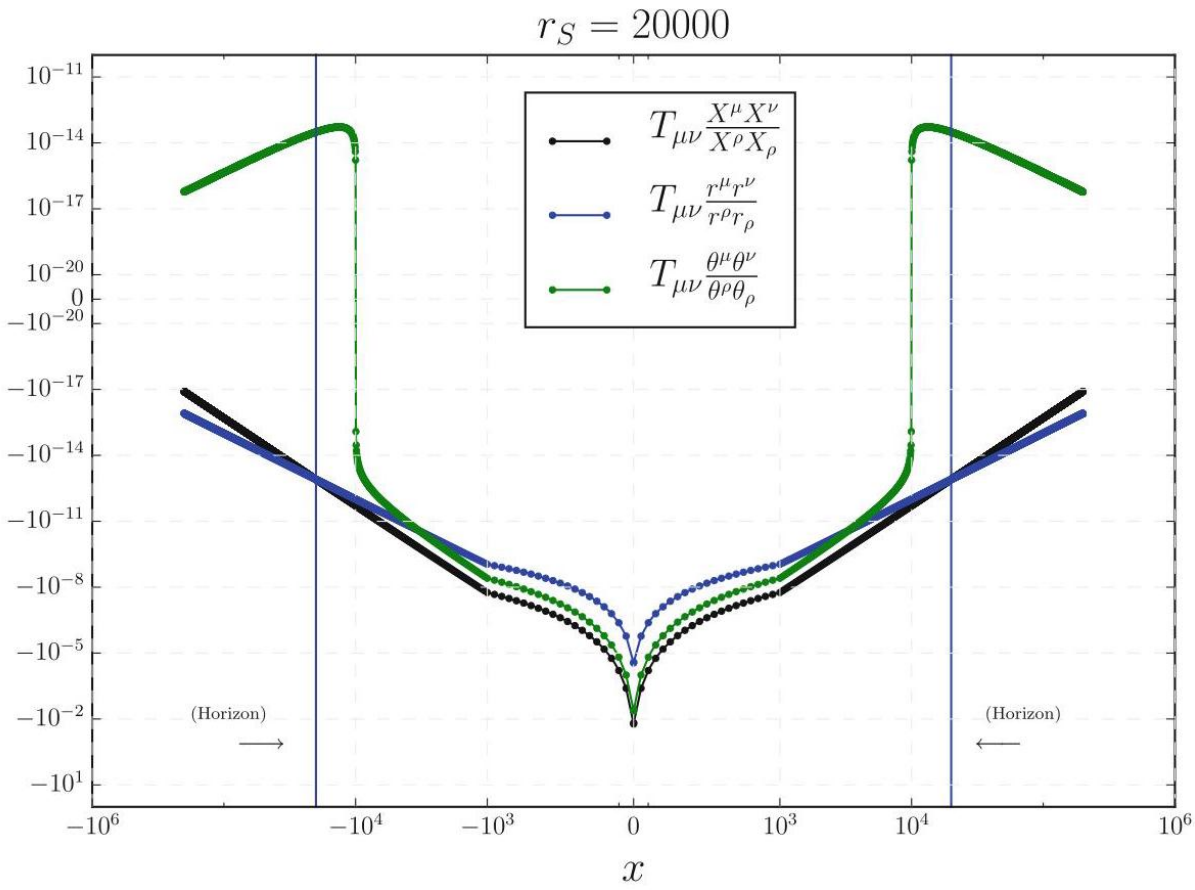

Fig. 3 The stress energy tensor of the effective metric ${}^{(0)}\tilde{g}_{\mu\nu}(x)$. This plot corresponds to $\delta x = \ell_{\rm Pl}$, namely, $s = 1$. (Reproduced from reference [18])

图 3 有效度量 ${}^{(0)}\tilde{g}_{\mu\nu}(x)$ 的应力能量张量。本图对应 $\delta x = \ell_{\rm Pl}$，即 $s = 1$。(转载自参考文献 [18])

Covariance

协变性

Since the quantizations we have considered are canonical, it may not appear obvious that the results are covariant in the traditional sense. For instance, the polymerization technique affects spatial variables that are slicing dependent. This has led to criticisms of our work [19].

由于我们研究的是正则量子化，其结果在传统意义上是否具有协变性并不显然。例如，聚合化技术会依赖于切片选取影响空间变量，这已经引发了对我们工作的批评 [19]。

An aspect that has to be pointed out is that we are redefining the constraints in order to have a Lie algebra between them. Any re-definition of variables is bound to have problems in certain points of phase space described in certain coordinates and may therefore lead to a non-equivalent quantization. We believe this is inevitable and a reasonable expectation.

必须指出的一点是，我们为了让约束之间满足李代数结构对约束做了重新定义。任何变量重定义在特定坐标描述的相空间某些点上都必然存在问题，因此可能得到不等价的量子化。我们认为这是不可避免的，也是合理的预期。

One way of checking covariance is to show that the resulting line elements from the space-time metrics constructed as Dirac observables are invariant. This was explored in some detail in [20]. Here we just show an example to give the flavor of the calculations involved, we refer to the cited reference for more details. Let us consider stationary foliations, like the Painlevé-Gullstrand or Eddington-Finkelstein coordinates. The choice of functional parameter $K_\varphi(x) = \kappa_\varphi(x)$ will determine the foliation. For convenience, we introduce a function $F(x_j)$ such that $\sin(\rho_j \alpha_\varphi(x_j)) = F(x_j)$ with $F(x_j) \in [-1,1]\,\forall x_j$ and therefore, with the notation $F(x_j) \equiv F_j$, and similarly for other parameters and operators, as we discussed before. Each choice of F_j corresponds to a different foliation, for instance, $F_j = \rho_j\sqrt{r_S/\sqrt{E_j^x}}$ leads to ingoing Painlevé-Gullstrand form of the metric and $F_j = \rho_j r_S/\sqrt{E_j^x\left(1+r_S/\sqrt{E_j^x}\right)}$ to ingoing Eddington-Finkelstein coordinates. The space-time metric is given by the operator,

检验协变性的一种方法是,证明构造为狄拉克可观测量的时空度量给出的线元具有不变性。文献 [20] 已经对此做了详细探讨，此处我们仅举例说明相关计算的思路，更多细节参见该引用文献。考虑定常叶化, 比如潘勒韦-古尔斯德兰坐标或爱丁顿-芬克尔斯泰因坐标, 函数参数 $K_\varphi(x) = \kappa_\varphi(x)$ 的选取决定叶化。为方便起见，我们引入函数 $F(x_j)$ 满足 $\sin(\rho_j\alpha_\varphi(x_j)) = F(x_j)$, 其中 $F(x_j) \in [-1,1]\,\forall x_j$, 因此采用记号 $F(x_j) \equiv F_j$, 其他参数与算符同理, 如我们之前所述。F_j 的每一种选取对应不同的叶化, 例如 $F_j = \rho_j\sqrt{r_S/\sqrt{E_j^x}}$ 给出内向潘勒韦-古尔斯德兰形式的度量, $F_j = \rho_j r_S/\sqrt{E_j^x\left(1+r_S/\sqrt{E_j^x}\right)}$ 对应内向爱丁顿-芬克尔斯泰因坐标。时空度量由如下算符给出:

$$\widehat{N}_F(x_j) = \sqrt{1+\frac{F_j^2}{\rho_j^2} - \frac{r_S}{\sqrt{\widehat{E}_j^x}}}, \tag{70}$$

$$\widehat{N}_F^x(x_j) = \frac{2F_j}{\rho_j}\frac{\sqrt{\widehat{E}_j^x}}{\left(\widehat{E}_j^x\right)'}\widehat{N}_F(x_j), \tag{71}$$

$$\hat{g}_{xx}^F(x_j) = \frac{\left(\left(\widehat{E}_j^x\right)'\right)^2}{4\widehat{E}_j^x}\widehat{N}_F(x_j)^{-2}, \tag{72}$$

$$\hat{g}_{tt}^F(x_j) = -1 + \frac{\hat{r}_S}{\sqrt{\widehat{E}_j^x}}, \tag{73}$$

$$\hat{g}_{tx}^F(x_j) = \hat{g}_{xx}(x_j)\,\widehat{N}_F^x(x_j). \tag{74}$$

In terms of this operator, we consider the length of a polygonal curve (t,x) described by a discrete set of points $[\ldots(t_j,x_j),(t_{j+1},x_{j+1})\ldots]$ where $\sqrt{\widehat{E}_j^x}\left|\vec{k},M\right\rangle = \ell_{\text{Planck}}\sqrt{k_j}\left|\vec{k},M\right\rangle = (|j|+j_0)\,\ell_{\text{Planck}}\left|\vec{k},M\right\rangle = x_j\left|\vec{k},M\right\rangle$ and $\hat{t}(x_j)\left|\vec{k},M\right\rangle = t(x_j)\left|\vec{k},M\right\rangle$. One can obtain more general ones combining these. The reason for talking about polygonal curves in space-time arises in that space is discrete. Their length can be written as,

基于该算符，我们考虑由离散点集 $[\ldots(t_j,x_j),(t_{j+1},x_{j+1})\ldots]$ 描述的多边形曲线 (t,x)，其中满足 $\sqrt{\widehat{E^x_j}}\left|\vec{k},M\right\rangle=\ell_{\text{Planck}}\sqrt{k_j}\left|\vec{k},M\right\rangle=(|j|+j_0)\,\ell_{\text{Planck}}\left|\vec{k},M\right\rangle=x_j\left|\vec{k},M\right\rangle$ 和 $\hat{t}\,(x_j)\left|\vec{k},M\right\rangle=t\,(x_j)\left|\vec{k},M\right\rangle$。组合这些构造即可得到更一般的曲线。在时空层面讨论多边形曲线的原因是空间本身是离散的。多边形曲线的长度可写为:

$$\left(\widehat{\Delta s_j}\right)^2=g_{ab}\left(\widehat{t_j},x_j\right)\widehat{\Delta x^a_j}\,\widehat{\Delta x^b_j}, \tag{75}$$

with $\widehat{\Delta x^0_j}=\hat{t}_{j+1}-\hat{t}_j=\widehat{\Delta t}_j$ and $\widehat{\Delta x^1_j}=\hat{x}_{j+1}-\hat{x}_j=\widehat{\Delta x}_j$.

其中 $\widehat{\Delta x^0_j}=\hat{t}_{j+1}-\hat{t}_j=\widehat{\Delta t}_j$ 且 $\widehat{\Delta x^1_j}=\hat{x}_{j+1}-\hat{x}_j=\widehat{\Delta x}_j$。

It is straightforward to show that the resulting expression is invariant when one chooses different F_j functions that correspond to different slices. Details can be seen in [20]. We have also studied the covariance of several curvature scalars: the Ricci and the Kretschmann scalars, and the scalar obtained by contracting the Weyl tensor with itself. We checked that in the approximation where x_j is treated as a continuous variable, which allows to use derivatives instead of finite differences, these scalars do not depend on the choice of the gauge function. Notice that the discreteness of the metric was still taken into account given the fact that $\left(\widehat{E^x}\right)'$ is always described by finite differences as was done for instance in equation (58-61) for Painlevé-Gullstrand.

不难证明，当选择对应不同切片的不同 F_j 函数时，所得表达式具有不变性，具体细节可见文献 [20]。我们还研究了多个曲率标量的协变性: 里奇标量、克雷奇曼标量，以及外尔张量自缩并得到的标量。我们验证了，在将 x_j 视为连续变量、从而可使用导数代替有限差分的近似下，这些标量不依赖于规范函数的选取。需要注意的是，我们仍然考虑了度规的离散性，因为正如潘勒韦-古尔斯 strand 例子的式 (58-61) 中所做的那样，$\left(\widehat{E^x}\right)'$ 始终是通过有限差分描述的。

Of course, this is just a check of covariance, and it is rather difficult to give a complete proof, since that would require evaluating all possible tensors computed from the metric and showing that they transform appropriately. But the straightforward nature of the above computations does not suggest any immediate problems in the construction of tensors from the metric and their transformation laws.

当然，这只是对协变性的一项验证，很难给出完整证明，因为完整证明需要计算所有由度规得到的张量，并证明它们满足正确的变换规则。但上述计算的直观推导过程表明，从度规构造张量并推导其变换规律不存在直接的问题。

Extension to Charged Black Holes

带电黑洞的推广

The above constructions can be extended to charged black holes. This was studied in reference [17]. There a gauge was chosen in which the electric field gets completely determined by the geometric variables. The resulting theory has a Hamiltonian constraint that differs by one term from the one we consider here, which is proportional to the charge squared. The kinematical Hilbert space remains the same, and one can proceed to find solutions to the Hamiltonian constraint, which still retains the same properties in the sense

of not changing the $\vec{k}$ valences when acting on a state. One can construct the metric as a Dirac observable and just like in the cases we discussed, demanding that it be a well-defined self-adjoint operator requires restricting the range in the k_j ' s, and this leads to the elimination of the singularity. This is true in the usual, extremal, or super-extremal case. In the latter, the operator remains self-adjoint until one hits the singularity, so the number of points to remove to ensure self-adjointness is smaller than in the regular case. The naked singularity present in the super-extremal case is therefore removed.

上述构造可以推广至带电黑洞，相关研究已见于文献 [17]。该研究选定了一种规范，其中电场完全由几何变量确定。所得理论的哈密顿约束与本文讨论的约束相比仅差一项，该项与电荷平方成正比。运动学希尔伯特空间保持不变，我们可以继续寻找哈密顿约束的解；该约束仍保留原有性质，即作用在态上时不会改变 $\vec{k}$ 价。我们可以将度规构造为狄拉克可观测量，且与本文讨论的情形相同，要求度规是良定义的自伴算子需要限制 k_j 的取值范围，这就会消除奇点。这一结论对常规、极端或超极端情形均成立。在超极端情形下，算子在到达奇点前始终保持自伴，因此为保证自伴性需要移除的点数量少于常规情形，超极端情形下存在的裸奇点因此被消除。

The weak gravity conjecture [21] claims that in any scheme involving gravitation and other interactions, naked singularities appear unless one guarantees that gravity is the weaker interaction. Since loop quantum gravity does not seem to put limits on the strength of the electromagnetic force, it has been suggested that this could be problematic due to the emergence of naked singularities [22]. The fact that in super extremal Reissner-Nordstrom, the naked singularity is removed indicates that the above objection is not necessarily true. In fact, some of the solutions used to demonstrate the weak gravity conjecture are in fact based on Wick rotations of Reissner-Nordstrom space-times [23]. Further research is needed in loop quantum gravity to probe all the issues involved, as the resulting space-times might be unstable [32].

弱引力猜想 [21] 指出，在任何包含引力与其他相互作用的理论框架中，只有保证引力是更弱的相互作用才会产生裸奇点。由于圈量子引力似乎并未对电磁力的强度施加限制，有观点认为裸奇点的出现会带来问题 [22]。超极端赖斯纳-努德斯特伦解中的裸奇点被消除这一事实表明，上述反对意见不一定成立。事实上，部分用于证明弱引力猜想的解本身就是基于赖斯纳-努德斯特伦时空的威克旋转得到的 [23]。圈量子引力仍需进一步研究才能探究所有相关问题，因为所得时空可能是不稳定的 [32]。

Some Observational Consequences

一些观测结果推论

Black hole space-times, when perturbed, admit modes of vibration, the so-called quasinormal modes (QNMs). They appear, for instance, during the ringdown regime of the final black hole after merging of its progenitors. They are gravitational waves of complex frequencies emitted outward to infinity and inwards toward the horizon. The imaginary part of the frequencies results in a decrease of the amplitude of the gravitational waves with time. Besides, in Einstein's theory, they only carry information about the mass, charge, and angular momentum of the black hole. Hence, they can be used as a probe to falsify theories.

受扰动的黑洞时空存在振动模式，即所谓的准正则模式 (QNM)。例如，它们会出现在前身黑洞并合后最终黑洞的铃宕阶段。这类模式是向外辐射至无穷远、向内落入事件视界的复频率引力波。频率的虚部导致引力波振幅随时间衰减。此外，在爱因斯坦理论中，准正则模式仅携带黑洞质量、电荷与角动量信息。因此，可用准正则模式作为证伪其他理论的探针。

These quasinormal frequencies are studied within the framework of perturbation theory of black hole space-times. In the case of the Schwarzschild black hole, the gauge invariant perturbations were originally introduced in Refs. [24, 25], and their gauge invariant formulation in Ref. [26]. They can be divided into two sectors according to their polarity: axial and polar perturbations. Their equations of motion are similar to the ones of a massless Klein-Gordon field (These equations are derived assuming the Einstein equations on a generic spherically symmetric background with vanishing Einstein tensor. The loop quantum gravity effects we will discuss stem from modifications of the background. There could be additional effects due to modifications of the Einstein equations themselves, we are ignoring these as a first analysis of the problem.). After factoring out the time and angular dependencies (the background geometries are static and spherically symmetric), the radial parts $\psi_{\tilde{\omega},\ell}(r)$ satisfy the equations of motion

这些准正则频率是在黑洞时空微扰理论的框架下开展研究的。针对史瓦西黑洞，规范不变微扰最早由文献 [24,25] 引入，其规范不变表述见文献 [26]。根据偏振性可将其分为两类: 轴向微扰和极向微扰。二者的运动方程均与无质量克莱因-戈登方程形式相似 (这些方程的推导基于: 爱因斯坦张量为零的一般球对称背景满足爱因斯坦方程。本文讨论的圈量子引力效应源自背景修正，作为问题的初步分析，我们忽略了爱因斯坦方程本身修正带来的额外效应)。分离时间和角度依赖项后 (背景几何为静态球对称)，径向部分 $\psi_{\tilde{\omega},\ell}(r)$ 满足运动方程

$$\frac{\partial^2\psi_{\tilde{\omega},\ell}}{\partial r_*^2}+\left[\tilde{\omega}^2-V_\ell(r)\right]\psi_{\tilde{\omega},\ell}=0, \tag{76}$$

where ℓ is the mode number associated to the spherical harmonic $Y_{\ell m}(\theta,\phi)$, $\tilde{\omega}$ is the (dimensionful) frequency, $V_\ell(r)$ an effective potential, and r_* is the tortoise coordinate defined as

其中 ℓ 是对应球谐函数的模式数，$Y_{\ell m}(\theta,\phi)$, $\tilde{\omega}$ 是 (量纲化) 频率，$V_\ell(r)$ 是有效势，r_* 是定义如下的龟坐标

$$\mathrm{d}r_*=\sqrt{\frac{F(r)}{G(r)}}\mathrm{d}r. \tag{77}$$

Here, $F(r)$ and $G(r)$ are some of the components of the line element of the spacetime that we can write as

在此，$F(r)$ 和 $G(r)$ 是时空线元的若干分量，我们可以将线元写为

$$\mathrm{d}s^2=-G(r)\,\mathrm{d}t^2+F(r)\,\mathrm{d}r^2+H(r)\,\mathrm{d}\Omega^2. \tag{78}$$

QNMs of black hole space-times, as originally proposed in Ref. [27], are those solutions to the radial equation (76) with boundary conditions

正如文献 [27] 最初提出的，黑洞时空的准正则模式是径向方程 (76) 满足如下边界条件的解

$$\psi_{n,\ell}(r) \propto e^{-i\widetilde{\omega}_{n,\ell} r_*} \quad r_* \to +\infty$$

$$\psi_{n,\ell}(r) \propto e^{i\widetilde{\omega}_{n,\ell} r_*} \quad r_* \to -\infty. \tag{79}$$

The resulting frequencies $\widetilde{\omega}_{n,\ell}$ belong to a discrete subset of imaginary numbers, with the imaginary part of $\widetilde{\omega}_{n,\ell}$ being positive. In this way, QNMs will dissipate in time.

得到的频率 $\widetilde{\omega}_{n,\ell}$ 属于虚数的离散子集，且 $\widetilde{\omega}_{n,\ell}$ 的虚部为正，因此准正则模式会随时间耗散。

In the case of axial perturbations, the potential has the form

对于轴向微扰，势的形式为

$${}^{(a)}V_{\ell}(r) = G(r)\left[\frac{\ell(\ell+1)}{H(r)} - R(r)\right] \tag{80}$$

where

其中

$$R(r) = \frac{2}{H(r)} + \frac{1}{F(r)}\left(\frac{G'(r)H'(r)}{4G(r)H(r)} - \frac{F'(r)H'(r)}{4F(r)H(r)} - \frac{3[H'(r)]^2}{4H^2(r)} + \frac{H''(r)}{2H(r)}\right), \tag{81}$$

with the primes denoting derivative with respect to r . For the polar perturbations, the potential is

撇号表示对 r 求导。对于极向微扰，势为

$${}^{(p)}V_{\ell}(r) = \frac{G(r)(\ell-1)^2(\ell+2)^2}{\lambda_{\ell}(r)^2}\left[\frac{(\ell-1)(\ell+2)+2}{H(r)} + R(r)\right. \tag{82}$$

$$\left. + \frac{H(r)R(r)^2}{(\ell-1)^2(\ell+2)^2}\left((\ell-1)(\ell+2) + \frac{H(r)R(r)}{3}\right)\right],$$

with

其中

$$\lambda_{\ell}(r) = (\ell-1)(\ell+2) + H(r)R(r). \tag{83}$$

To compute the complex frequencies of these QNMs, one can use a WKB method. Here, one needs to solve for $\widetilde{\omega}_{n,\ell}$ in the equation

要计算这些准正则模式的复频率，可以采用 WKB 方法。此时需要求解方程中 $\widetilde{\omega}_{n,\ell}$ ，方程形式为

$$\widetilde{\omega}^2_{n,\ell} = V_\ell(\tilde{r}) - \sqrt{-2V''_\ell(\tilde{r})}\left[\left(n+\frac{1}{2}\right) + \sum_{i=2}^{N}\Lambda^{(i)}_{n,\ell}(\tilde{r})\right]. \tag{84}$$

The functions $\Lambda^{(i)}_{n,\ell}(\tilde{r})$ codify high-order WKB corrections, which depend on $\widetilde{\omega}_{n,\ell}$ itself and on the derivatives of the corresponding potential evaluated on its maximum located at $V'_\ell(\tilde{r}) = 0$. Closed-form expressions for $\Lambda^{(i)}_{n,\ell}(\tilde{r})$ can be found in Refs. [28, 29]. Interestingly, in the case of the Schwarzschild black hole, the quasinormal spectrum of axial and polar perturbations is isospectral, namely they agree, despite their potential being different. However, the origin of this agreement was already noted in Ref. [27] and explained in detail in [30] as a consequence of the covariance of Eq. (76) under Darboux transformations.

函数 $\Lambda^{(i)}_{n,\ell}(\tilde{r})$ 编码了 WKB 的高阶修正，修正取决于 $\widetilde{\omega}_{n,\ell}$ 本身，以及对应势在其最大值 $V'_\ell(\tilde{r}) = 0$ 处的导数。$\Lambda^{(i)}_{n,\ell}(\tilde{r})$ 的闭式表达式可在文献 [28,29] 中找到。值得注意的是，对于史瓦西黑洞，轴向微扰和极向微扰的准正则谱是同谱的，即尽管二者的势不同，准正则谱却完全一致。这种一致性的起源在文献 [27] 中就已经被指出，并在文献 [30] 中得到了详细解释: 其本质是方程 (76) 在达布变换下协变性的结果。

However, in the case of the effective geometries discussed in this chapter, a detailed calculation in Ref. [31] shows not only that their quasinormal frequencies deviate from the classical black hole but also that isospectrality is violated. Nevertheless, these deviations are small for macroscopic black holes, since they decrease fast with the radius of the horizon. For instance, if one chooses in Eq. (62) the parameter $\delta x = x_0$, those deviations decrease with the power $(r_S/\ell_{\rm Pl})^{-2/3}$, while for $\delta x = \ell^2_{\rm Pl}/(2r_0)$, they decrease as $(r_S/\ell_{\rm Pl})^{-4/3}$, for any choice of n and ℓ. In Table 1, we show the numerical values of the dimensionless quasinormal frequencies, namely $\omega_{n\ell} = (r_S/2G)\,\widetilde{\omega}_{n,\ell}$, as is usual in the literature.

但就本章所讨论的有效几何而言，文献 [31] 中的详细计算不仅表明它们的准正则频率与经典黑洞的准正则频率存在偏差，还表明等谱性遭到了破坏。不过，这些偏差在宏观黑洞中很小，因为偏差会随着视界半径增大而快速衰减。例如，若在式 (62) 中选取参数 $\delta x = x_0$，这些偏差会以幂次 $(r_S/\ell_{\rm Pl})^{-2/3}$ 衰减；而对任意选取的 n 和 ℓ，当取值为 $\delta x = \ell^2_{\rm Pl}/(2r_0)$ 时，偏差会以 $(r_S/\ell_{\rm Pl})^{-4/3}$ 的形式衰减。如表 1 所示，我们给出了无量纲准正则频率的数值，即文献中常用的 $\omega_{n\ell} = (r_S/2G)\,\widetilde{\omega}_{n,\ell}$。

Recently, there have also been interesting investigations of alternative black hole models in loop quantum gravity in terms of quasinormal modes [33], also including the possibility of observations with the Event Horizon Telescope [34].

近年来，在圈量子引力框架下也有不少基于准正则模对另类黑洞模型开展的有趣研究 [33]，其中还包括利用事件视界望远镜进行观测的可能性 [34]。

Mini-Superspace Approach: Kantowski-Sachs Models

微超空间方法: 坎托夫斯基-萨克斯模型

Another complementary approach for the quantization of black holes spacetimes, which usually focuses on singularity resolution, restricts the study to the region inside the horizon. This region is (classically) isometric to the (vacuum) Kantowski-Sachs cosmologies. The homogeneity of the spatial hypersurfaces allows

one to apply LQC quantization techniques. The literature on the topic is considerable (see, for instance, [5, 35-45, 47-49]). These models, due to homogeneity, have two kinematical, global degrees of freedom, corresponding to the independent components of the Ashtekar connection and the conjugate densitized triad, usually denoted by the conjugate pairs (c, p_c) and (b, p_b) , respectively. The Hamiltonian constraint involves the curvature of the connection, which in the quantum theory is written in terms of holonomies of the gravitational connection around suitable loops with a minimum non-zero area. The dynamics of the system has been studied in most of the literature by assuming an effective description.

黑洞时空量子化的另一种互补方法通常聚焦于奇点解决，它将研究限制在视界内部区域。该区域 (经典层面) 等距于 (真空) 坎托夫斯基-萨克斯宇宙学。空间超曲面的齐次性使得人们可以应用 LQC 量子化技术。关于该主题的研究文献相当丰富 (例如参见 [5, 35-45, 47-49])。由于齐次性，这些模型拥有两个运动学全局自由度，分别对应阿希特卡联络和共轭密化三分量标架的独立分量，通常用共轭对 (c, p_c) 和 (b, p_b) 分别表示。哈密顿约束包含联络曲率，在量子理论中，曲率是通过引力联络绕具有最小非零面积的合适回路的全纯联络表示的。现有大部分文献都通过假设有效描述研究了该系统的动力学。

Table 1 Quasinormal frequencies for the first overtones of axial and polar perturbations. In the first column, we show the results for the Schwarzschild black hole (due to isospectrality we do only include axial perturbations). In the second and third columns, we show the corresponding axial and polar frequencies of our effective geometry, respectively. They correspond to the choice $\delta x = x_0$ and for $r_S = 10^3 \ell_P$

表 1 轴向和极向扰动一阶泛音的准正规频率。第一列给出施瓦西黑洞的结果 (由于等谱性，我们仅包含轴向扰动)。第二列和第三列分别给出我们有效几何对应的轴向频率和极向频率。它们对应参数选择 $\delta x = x_0$ 和 $r_S = 10^3 \ell_P$

Quasinormal frequencies $\left(r_S = 10^3 \ell_P\right)$			
(n, ℓ)	Schwarzschild	Axial	Polar
(0,2)	0.74733225-0.17792806i	0.74736483-0.17720680i	0.74749081-0.17733983i
(1,2)	0.69322645-0.54811740i	0.69401982-0.54578773i	0.69407330-0.54597173i
(0,3)	1.19888658-0.18540612i	1.19894618-0.18468114i	1.19897954-0.18471131i
(1,3)	1.16528891-0.56259764i	1.16577313-0.56034440i	1.16577795-0.56043389i
(0,4)	1.61835676-0.18832792i	1.61841428-0.18758921i	1.61842820-0.18759958i
(1,4)	1.59326305-0.56866870i	1.59363598-0.56640627i	1.59364290-0.56643745i
(0,5)	2.02459062-0.18974103i	2.02464204-0.18899367i	2.02464917-0.18899817i
(1,5)	2.00444206-0.57163476i	2.00474707-0.56936206i	2.00475176-0.56937559i
(0,6)	2.42401964-0.19053169i	2.42406539-0.18977889i	2.42406933-0.18978122i
(1,6)	2.40714795-0.57329985i	2.40740646-0.57101967i	2.40740936-0.57102668i

Analysis of the effective equations of motion of these models shows that the singularity is replaced by a space-like, 3-dimensional transition surface. It separates a trapped and an anti-trapped region. They correspond to black hole and white hole regions, respectively. However, different approaches in the literature differ in the choice of the loops of the holonomies that regularize the effective Hamiltonian constraint, namely in the choice of two quantum parameters, denoted by δ_b and δ_c . The choices can be classified into three broad classes. In general, they are proportional to the (square root of) area gap Δ times a function, which can be different for each parameter. In [35,36,42] these functions are constant; in [5,45,47] they are chosen as functions of Dirac observables (functions on phase space constant along dynamical trajectories); and in [37-40,43,46,48]

they are more general functions on phase space (non-constant on dynamical trajectories). As was noted in Ref. [5], some of these choices have undesirable or puzzling features with no clear physical origin. With this motivation, and adopting the strategy in which δ_b and δ_c are chosen to be functions of Dirac observables, reference [5] suggests a judicious choice for these parameters where the area enclosed by the loops at the transition surface equals the area gap Δ of loop quantum gravity. As a result, the transition surface is always located at the Planck regime while there is an excellent agreement with classical general relativity in low-curvature regions. Moreover, reference [5] also extends the effective description to the asymptotic regions and shows that the effective metric is smooth across the horizon, the surface joining the exterior and interior regions.

对这些模型有效运动方程的分析表明，奇点被类空的三维过渡曲面取代。该曲面分隔了被俘获区域和反被俘获区域，二者分别对应黑洞区域和白洞区域。不过，现有文献中不同方法在正则化有效哈密顿约束的全纯回路选择上存在差异，具体来说就是两个量子参数的选择不同，记为 δ_b 和 δ_c 。这些选择可以大致分为三类。一般而言，它们与面积隙 Δ (的平方根) 成正比，再乘以一个函数，两个参数对应的函数可以不同。在文献 [35,36,42] 中，这些函数是常数；在 [5,45,47] 中，它们被取为狄拉克可观测量的函数 (即相空间中沿动力学轨迹不变的函数)；在 [37-40,43,46,48] 中，它们是相空间上更一般的函数 (沿动力学轨迹非常数)。正如文献 [5] 指出的，部分这类选择存在不合情理或令人困惑的特性，没有明确的物理起源。基于这一动机，同时采用 δ_b 和 δ_c 取为狄拉克可观测量函数的策略，文献 [5] 对这些参数给出了一个合理选择: 过渡表面处回路围成的面积等于圈量子引力的面积隙 Δ 。结果表明，过渡曲面始终位于普朗克区域，同时在低曲率区域与经典广义相对论高度吻合。此外，文献 [5] 还将有效描述扩展到渐近区域，证明有效度量在视界 (连接外部区域和内部区域的曲面) 上处处光滑。

The effective space-time line element of these geometries is given by the expression

这些几何的有效时空线元表达式如下

$$g_{ab}dx^a dx^b \equiv ds^2 = -N^2 dT^2 + \frac{p_b^2}{|p_c|\, L_o^2} dx^2 + |p_c| \left(d\theta^2 + \sin^2\theta d\phi^2 \right), \tag{85}$$

where L_o is the length of a fiducial cell introduced to avoid spurious divergencies due to the non-compactness of the spatial slicing, and N is the lapse function

其中 L_o 是为避免因空间切片非紧性产生伪发散而引入的基准胞元长度，N 是时移函数

$$N = \frac{\gamma p_c^{1/2} \delta_b}{\sin(\delta_b b)}, \tag{86}$$

with γ the Immirzi parameter (we chose it to be equal one but we leave it here explicitly). The effective Hamiltonian (constraint) of the system is

其中 γ 是伊米尔齐参数 (我们已将其取为 1，但仍在此明确写出)。系统的有效哈密顿 (约束) 为

$$H_{\text{eff}}[N] = -\frac{1}{2G\gamma} \left[2\frac{\sin(\delta_c c)}{\delta_c} p_c + \left(\frac{\sin(\delta_b b)}{\delta_b} + \frac{\gamma^2 \delta_b}{\sin(\delta_b b)} \right) p_b \right]. \tag{87}$$

One can easy see that in the classical limit $\delta_b \to 0$ and $\delta_c \to 0$, one recovers the classical limit of the lapse function N and the classical Hamiltonian. The dynamical equations for the phase space variables are

不难看出，在经典极限 $\delta_b \to 0$ 和 $\delta_c \to 0$ 下，我们可以重新得到时移函数 N 的经典极限和经典哈密顿量。相空间变量的动力学方程为

$$\dot{b} = -\frac{1}{2}\left(\frac{\sin(\delta_b b)}{\delta_b} + \frac{\gamma^2 \delta_b}{\sin(\delta_b b)}\right), \ \dot{c} = -2\frac{\sin(\delta_c c)}{\delta_c}, \tag{88}$$

and

和

$$\dot{p}_b = \frac{p_b}{2}\cos(\delta_b b)\left(1 - \frac{\gamma^2 \delta_b^2}{\sin^2(\delta_b b)}\right), \ \dot{p}_c = 2p_c \cos(\delta_c c). \tag{89}$$

It is easy to integrate the Hamilton’s equations for b, c , and p_c , while we obtain the solution for p_b using the effective Hamiltonian constraint $H_{\text{eff}} \approx 0$ on shell. The solution is:

我们可以很容易积分得到 b, c 和 p_c 的哈密顿方程解，再利用壳有效哈密顿约束 $H_{\text{eff}} \approx 0$ 得到 p_b 的解，解如下:

$$\tan\left(\frac{\delta_c c(T)}{2}\right) = \mp\frac{\gamma L_o \delta_c}{8m} e^{-2T}, \tag{90}$$

$$p_c(T) = 4m^2\left(e^{2T} + \frac{\gamma^2 L_o^2 \delta_c^2}{64m^2} e^{-2T}\right), \tag{91}$$

$$\cos(\delta_b b(T)) = b_o \tanh\left(\frac{1}{2}\left(b_o T + 2\tanh^{-1}\left(\frac{1}{b_o}\right)\right)\right), \tag{92}$$

where

其中

$$b_o = \left(1 + \gamma^2 \delta_b^2\right)^{1/2} \tag{93}$$

and,

并且,

$$p_b(T) = -2\frac{\sin(\delta_c c(T))}{\delta_c}\frac{\sin(\delta_b b(T))}{\delta_b}\frac{p_c(T)}{\frac{\sin^2(\delta_b b(T))}{\delta_b^2} + \gamma^2}. \tag{94}$$

One should note that the triad p_c is bounded from below by $p_c|_{\min} = m\gamma L_o \delta_c$ in every effective spacetime, where

需要注意的是，在每个有效时空中，三元组 p_c 以 $p_c|_{\min} = m\gamma L_o \delta_c$ 为下界，其中

$$m := \left[\frac{\sin \delta_c c}{\gamma L_o \delta_c}\right] p_c, \tag{95}$$

is the mass of the black hole space-time. In consequence, these geometries are free of singularities. One can see that they define a transition surface from the trapped (black hole type) region to an anti-trapped (white hole type) region. The improved dynamics proposed in Ref. [5], where the minimum area conditions are imposed at this transition surface, after a detailed calculation, show that, in the large mass limit,

是黑洞时空的质量。因此，这些几何不存在奇点。可以看到它们定义了从俘获区 (黑洞型) 到反俘获区 (白洞型) 的过渡曲面。文献 [5] 提出的改进动力学在该过渡曲面上施加了最小面积条件，经过详细计算表明，在大质量极限下，

$$\delta_b = \left(\frac{\sqrt{\Delta}}{\sqrt{2\pi}\gamma^2 m}\right)^{1/3}, \; L_o\delta_c = \frac{1}{2}\left(\frac{\gamma\Delta^2}{4\pi^2 m}\right)^{1/3}. \tag{96}$$

Therefore, δ_b and δ_c are fixed once and for all to these values, even if one evaluates the effective geometry away from the transition surface.

因此，即使在远离过渡曲面的位置计算有效几何，δ_b 和 δ_c 也始终固定为这些值。

The resulting effective interior geometries can be given explicitly. They have some interesting properties. For instance, curvature invariants, evaluated at the transition surface, defined by $\dot{p}_c\,(T_{\mathcal{F}}) = 0$, have universal upper bounds that are mass-independent (in the large mass limit). Concretely, the (square of the) Ricci scalar has the asymptotic form:

最终得到的有效内部几何可以显式给出，它们具备若干有趣的性质。例如，由 $\dot{p}_c\,(T_{\mathcal{F}}) = 0$ 定义的过渡曲面上计算得到的曲率不变量存在不依赖质量的普适上界 (大质量极限下)。具体而言，里奇标量 (的平方) 具有渐近形式:

$$R^2\,(T_{\mathcal{F}}) = \frac{256\pi^2}{\gamma^4\Delta^2} + O\left(\left(\frac{\Delta}{m^2}\right)^{\frac{1}{3}} \ln\frac{m^2}{\Delta}\right); \tag{97}$$

the square of the Ricci tensor has the asymptotic form

里奇张量的平方具有渐近形式

$$R_{ab}R^{ab}\,(T_{\mathcal{F}}) = \frac{256\pi^2}{\gamma^4\Delta^2} + O\left(\left(\frac{\Delta}{m^2}\right)^{\frac{1}{3}} \ln\frac{m^2}{\Delta}\right); \tag{98}$$

the square of the Weyl tensor has the asymptotic form

外尔张量的平方具有渐近形式

$$C_{abcd}C^{abcd}\,(T_{\mathcal{F}}) = \frac{1024\pi^2}{3\gamma^4\Delta^2} + O\left(\left(\frac{\Delta}{m^2}\right)^{\frac{1}{3}} \ln\frac{m^2}{\Delta}\right); \tag{99}$$

and, consequently, the Kretschmann scalar $K = R_{abcd}R^{abcd}$ has the asymptotic form

因此，克雷奇曼标量 $K = R_{abcd}R^{abcd}$ 具有渐近形式

$$K(T_{\mathcal{F}}) = \frac{768\pi^2}{\gamma^4\Delta^2} + O\left(\left(\frac{\Delta}{m^2}\right)^{\frac{1}{3}} \ln\frac{m^2}{\Delta}\right). \tag{100}$$

Hence, the non-vanishing of the Ricci tensor and the Einstein equations imply that there is a nontrivial stress-energy tensor. Actually, Ref. [5] showed that this effective stress-energy tensor violates the strong energy conditions. Moreover, it decreases fast away from the transition surface. Hence, the effective geometries are in very good agreement with the classical geometries close to the past and future horizons.

由此，里奇张量非零结合爱因斯坦方程可得，存在非平凡的能动张量。实际上文献 [5] 已经证明，该有效能动张量违背强能量条件。此外，它会随远离过渡曲面快速衰减。因此，在靠近过去视界和未来视界的区域，有效几何与经典几何契合度非常高。

All these properties of the interior geometry of these effective Kruskal geometries are unique. In particular, the prescriptions in which δ_b and δ_c are chosen to be constant, either they give results sensitive to the value of the fiducial parameter L_o or the curvature at the transition surface has no upper universal bounds [35, 36, 41, 42, 44, 45, 47] . Other prescriptions where they are chosen to be functions of Dirac observables show a similar issue with curvature invariants at the transition surface, and they also give a white hole geometry with a very large mass compared to the black hole mass [37, 38, 43, 46, 48] . The physical origin of this large difference is still unclear. Finally, the choices for δ_b and δ_c that involve more general functions on phase space, so far, either trigger large quantum corrections at regions where one does not expect such deviations from the classical theory or the improved dynamics conditions are no longer valid, and they cannot be trusted (see [5] for details).

这些有效克鲁斯卡尔几何的内部几何的所有性质都是唯一的。具体来说，将 δ_b 和 δ_c 取为常数的方案，要么所得结果对基准参数 L_o 的取值敏感，要么过渡曲面处的曲率不存在普适上界 [35, 36, 41, 42, 44, 45, 47] 。将 δ_b 和 δ_c 取为狄拉克可观测量函数的其他方案，在过渡曲面的曲率不变量上也存在类似问题，且所得白洞几何质量远大于黑洞质量 [37, 38, 43, 46, 48] 。这种巨大差异的物理起源目前仍不清楚。最后，涉及相空间更广义函数来选取 δ_b 和 δ_c 的方案，到目前为止，要么会在原本预期不会偏离经典理论的区域引发大的量子修正，要么改进动力学条件不再成立，结果不可信 (细节见文献 [5])。

Moreover, Ref. [5] also introduced the extension of the effective geometries to the exterior region. They suggest adopting the same spacetime foliation (i.e., a homogeneous slicing). However, the intrinsic metric of the hypersurfaces has Lorentzian signature (they are not space-like as in the interior). Therefore, the signature of the internal space for the gravitational connection and triads also has signature -, +, + . This implies that the internal gauge group is now SU (1, 1) (rather than SU (2)). Keeping this difference in mind, the phase space variables for the exterior region can be obtained simply by making the substitutions

此外，文献 [5] 还将有效几何延拓到了外部区域。作者建议采用相同的时空叶分 (即齐次切片)。但超曲面的内蕴度量是洛伦兹号差 (不像内部那样是类空的)。因此，引力联络和三元组的内空间号差也变为负，+, + 。这意味着内规范群现在是 SU (1, 1) (而非 SU (2))。记住这一差异后，只需通过代换即可得到外部区域的相空间变量:

$$b \to i\tilde{b}, p_b \to i\widetilde{p}_b;\ c \to \tilde{c}, p_c \to \widetilde{p}_c. \tag{101}$$

The Hamiltonian constraint for the exterior region now has the form

外部区域的哈密顿约束现在形式为

$$\widetilde{H}_{\text{eff}}\left[\widetilde{N}\right]=-\frac{1}{2G\gamma}\left[2\frac{\sin\left(\delta_{\tilde{c}}\tilde{c}\right)}{\delta_{\tilde{c}}}\left|\widetilde{p}_{c}\right|+\left(-\frac{\sinh\left(\delta_{\tilde{b}}\tilde{b}\right)}{\delta_{\tilde{b}}}+\frac{\gamma^{2}\delta_{\tilde{b}}}{\sinh\left(\delta_{\tilde{b}}\tilde{b}\right)}\right)\widetilde{p}_{b}\right].$$

(102)

Hamilton's equations can be obtained and also easily integrated. The resulting exterior metric admits a closed-form expression given by

可以推导出哈密顿方程，且极易积分。所得外部度规存在闭合形式表达式，由下式给出

$$\tilde{g}_{ab}dx^{a}dx^{b}=\tilde{g}_{tt}dt^{2}+\tilde{g}_{rr}dr^{2}+\widetilde{R}^{2}d\omega^{2},\tag{103}$$

with

其中

$$\tilde{g}_{tt}=-\left(\frac{r}{r_{S}}\right)^{2\varepsilon}\frac{\left(1-\left(\frac{r_{S}}{r}\right)^{1+\varepsilon}\right)\left(2+\varepsilon+\varepsilon\left(\frac{r_{S}}{r}\right)^{1+\varepsilon}\right)^{2}\left((2+\varepsilon)^{2}-\varepsilon^{2}\left(\frac{r_{S}}{r}\right)^{1+\varepsilon}\right)}{16\left(1+\frac{\delta_{\tilde{c}}^{2}L_{0}^{2}\gamma^{2}r_{S}^{2}}{16r^{4}}\right)(1+\varepsilon)^{4}},$$

(104)

$$\tilde{g}_{rr}=\left(1+\frac{\delta_{c}^{2}L_{0}^{2}\gamma^{2}r_{S}^{2}}{16r^{4}}\right)\frac{\left(\varepsilon+\left(\frac{r}{r_{S}}\right)^{1+\varepsilon}(2+\varepsilon)\right)^{2}}{\left(\left(\frac{r}{r_{S}}\right)^{1+\varepsilon}-1\right)\left(\left(\frac{r}{r_{S}}\right)^{1+\varepsilon}(2+\varepsilon)^{2}-\varepsilon^{2}\right)},\tag{105}$$

and

且

$$R^{2}\;:=\;\widetilde{p}_{c}=4m^{2}\left(e^{2T}+\frac{\gamma^{2}L_{0}^{2}\delta_{\tilde{c}}^{2}}{64m^{2}}e^{-2T}\right)\equiv r^{2}\left(1+\frac{\gamma^{2}L_{0}^{2}\delta_{\tilde{c}}^{2}r_{S}^{2}}{16r^{4}}\right),\tag{106}$$

where $r_{S}\;:=\;2m$ and $1+\varepsilon\;:=\;\left(1+\gamma^{2}\delta_{\tilde{b}}^{2}\right)^{\frac{1}{2}}$.

式中 $r_{S}\;:=\;2m$ 和 $1+\varepsilon\;:=\;\left(1+\gamma^{2}\delta_{\tilde{b}}^{2}\right)^{\frac{1}{2}}$。

This metric has several interesting properties. For instance, in the limit in which $\delta_{\tilde{c}}\to 0$ and $\delta_{\tilde{b}}\to 0$, one recovers the Schwarszchild metric in its standard form. Besides, it is asymptotically flat, but the fall-off conditions are not the standard ones [62]. Here, several curvature scalars computed out of the Riemann tensor (in particular the Krestchamnn scalar) decay as r^{-4} rather than r^{-6} , as in the classical case. Despite this non-standard asymptotic behavior, quantities like the ADM, Ricci, and horizon energies are well defined, and they agree up to small corrections (in the large m limit). Moreover, one can actually check that, even for microscopic black holes with masses, a few orders of magnitude larger than the Planck mass, deviation from

the classical theory appears at distances many orders of magnitude beyond the current Hubble horizon size 5Gpc $\sim 10^{61}\ell_{Pl}$ (see [49] for details).

该度规具有几个值得注意的性质: 例如，当 $\delta_{\tilde{c}} \to 0$ 和 $\delta_{\tilde{b}} \to 0$ 取极限时，我们可以得到标准形式的施瓦西度规。此外，该度规是渐近平直的，但它的衰减条件并非标准衰减条件 [62]。此处，由黎曼张量计算得到的多个曲率标量 (尤其是克里施曼标量) 按 r^{-4} 衰减，而非经典情形下的 r^{-6} 衰减。尽管这种渐近行为是非标准的，但 ADM 质量、里奇能量和视界能量这些物理量都是定义良好的，且在大 m 极限下，它们和经典结果只相差微小修正。此外我们还可以验证，即使是质量仅比普朗克质量高几个数量级的微型黑洞，其与经典理论的偏差也出现在远大于当前哈勃视界尺寸 5Gpc $\sim 10^{61}\ell_{Pl}$ 的距离处 (详见文献 [49])。

Finally, we would like to mention that the near-horizon geometry agrees very well with the classical one. By means of quantum fields propagating on static space-times and using Euclidean methods, one can easily calculate the temperature associated with the Killing horizon. The result (see Ref. [49]) is

最后我们需要指出，近视界面几何和经典几何吻合得很好。通过在静态时空上传播量子场，并使用欧几里得方法，我们可以很容易地计算出基灵视界对应的温度，结果如下 (参见文献 [49])

$$T_{\mathrm{H}} = \frac{\hbar}{8\pi k_B m}\frac{1}{(1+\varepsilon_m)}, \tag{107}$$

where k_B is the Boltzmann constant, and

其中 k_B 是玻尔兹曼常数，且

$$\varepsilon_m = \frac{1}{256}\left(\frac{\gamma\Delta^{\frac{1}{2}}}{\sqrt{2\pi}m}\right)^{8/3}. \tag{108}$$

This correction is tiny, even for microscopic black holes. For instance, for a black hole of $10^6 M_{\mathrm{Pl}}$, the correction to the Hawking temperature is as small as 10^{-21} , while for a solar mass black hole, its value is of the order of 4×10^{-106} .

这种修正非常微小，即使对微型黑洞而言也是如此。例如，对于质量为 $10^6 M_{\mathrm{Pl}}$ 的黑洞，霍金温度的修正仅为 10^{-21} ；而对于太阳质量的黑洞，修正的量级约为 4×10^{-106} 。

We would like to conclude this section by mentioning that, although these models have been studied mainly within the effective dynamics approximation, some few contributions have been focused on the genuine quantum theory. For instance, [41] explored the solutions to the difference equation proposed in [35]. In [42], after a reduced phase space quantization, the authors compute the physical states and derive the effective dynamics of semi-classical states. Besides, Ref. [50,51] shows that the spectrum of the mass operator is discrete with a minimum non-vanishing eigenvalue, indicating that the final fate of evaporation can be a stable black hole remnant. Moreover, [52] explores for the first time several properties of physical quantum states of the model proposed in [5].

在本节的最后我们要说明，尽管这些模型主要是在有效动力学近似下开展研究，但也有少量研究工作关注真正的量子理论。例如，文献 [41] 研究了文献 [35] 中提出的差分方程的解。文献 [42] 在约化相空间量子化后，计算了物理态并推导了半经典态的有效动力学。此外，文献 [50,51] 表明，质量算符的谱是离散的，且存在最小非零本征值，这说明蒸发的最终结果可以是一个稳定的黑洞残余。此外，文献 [52] 首次研究了文献 [5] 中提出的模型的物理量子态的若干性质。

Besides, other proposals have been motivated or derived from the full theory and include additional corrections into the effective Hamiltonian constraint. This is the case, for instance, of Refs. [53-56]. These modifications affect mainly the interior region beyond the transition surface. There, one does not recover a classical white hole geometry. However, there is agreement with respect to singularity resolution and the right semi-classical physics close to the black hole horizon.

此外，还有其他源自完整理论或受完整理论启发提出的方案，这些方案在有效哈密顿约束中引入了额外修正，例如文献 [53-56] 就是这类情况。这些修改主要影响相变面内侧的区域: 在该区域我们无法得到经典的白洞几何，但在奇点消解以及黑洞视界附近的正确半经典物理方面，这些修改和现有结论是一致的。

Conclusions

结论

We have given an overview of some of the most relevant contributions on spherically symmetric loop quantum gravity, which is based on assuming spherical symmetry in the classical theory and then quantizing the resulting reduced model. We start the discussion with models where the slicings are inhomogeneous outside black holes and that can penetrate the interior and go over the region where the singularity used to be in the classical theory and be continued beyond there smoothly. The singularity is naturally avoided if one demands that the metric be a well-defined self-adjoint operator. We also discussed the charged case, potentially observable effects by studying quansinormal ringing and the covariance of the approach. It should be noted that this treatment completes the Dirac quantization of the system and analyzes its semi-classical properties in terms of Dirac observables. It is the first such treatment in quantum general relativity in a field theoretic context. Some recent proposals, like [57] discuss a covariant effective description where no abelianization of the constraint is required, provided one adopts a partial polymerization of geometrical variables (in this approach, an extension where all connection variables are polymerized is still unknown). Moreover, in the last years, several models of collapse, discussing black hole formation and even evaporation, have been proposed in [58-61]. The studies adopt numerical approaches that allow them to probe the formation of a dynamical horizon (black hole type) and critical phenomena [58,59]. Besides, in Ref. [60, 61], the authors show that once the matter reaches the high curvature region, it bounces, forming a shock wave that eventually evaporates the black hole in a time that is proportional to the square of its mass. A different conclusion is reached in [63]. Additional models for collapse without local degrees of freedom can be seen in [64].

我们概述了球对称圈量子引力领域一些最具相关性的研究成果，这类研究的基础是在经典理论中假设球对称性，再对约化后的模型进行量子化。我们首先讨论的模型满足: 切片在黑洞外是非均匀的，可穿透黑洞内部，覆盖经典理论中原先存在奇点的区域，并能平滑延伸至奇点之外。若要求度规是定义良好的自伴算子，奇点就会自然被消除。我们还讨论了带电情形、通过准正则 ringing 研究的潜在可观测效应，以及该方法的协变性。需要说明的是，这套处理完成了系统的狄拉克量子化，并基于狄拉克可观测量分析了模型的半经典性质，这是量子广义相对论在场论框架下首次完成这类处理。近期还有一些研究提案，比如文献 [57] 讨论了协变有效描述: 只要对几何变量采用部分聚合，就不需要对约束做阿贝尔化 (该方法目前还不清楚如何推广到全部联络变量都聚合的情况)。此外，近年来文献 [58-61] 提出了若干坍缩模型，讨论了黑洞形成乃至蒸发过程。这些研究采用数值方法，可以探测动力学视界 (黑洞型) 的形成和临界现象 [58,59]。另外，在文献 [60, 61] 中，作者表明当物质到达高曲率区域后会发生反弹，形成冲击波，最终使黑洞在与其质量平方成正比的时间内蒸发。文献 [63] 则得出了不同的结论。不包含局部自由度的其他坍缩模型可见文献 [64]。

We have also discussed other approaches that exploit the simplicity of homogeneous slicings in spherical symmetry. In this case, black hole dynamics can be described by means of few global degrees of freedom. Some of the most recent treatments introduce novel choices of the length of the plaquettes of the loops resulting on effective geometries that solve some of the problems found in previous proposals. Most of the models agree in some of the physical properties of the trapped interior region and singularity resolution, but the fate of the geometry beyond this quantum region is still a matter of debate.

我们还讨论了利用球对称下均匀切片简化性的其他研究方法。在这类方法中，黑洞动力学可以通过少数几个全局自由度描述。一些最新研究对格点圈的边长给出了新选择，得到的有效几何解决了此前提案中存在的部分问题。多数模型在俘获内部区域的部分物理性质和奇点消除方面结论一致，但量子区域之外几何的最终走向仍存在争议。

Acknowledgments This work was supported in part by Grant NSF-PHY-1903799, NSF-PHY- 2206557, funds of the Hearne Institute for Theoretical Physics, CCT-LSU, Pedeciba, Fondo Clemente Estable FCE 1 2019 1 155865 and the Spanish Government through the projects PID2020-118159GB-C43, PID2019-105943GB-I00 (with FEDER contribution), and the ”Operative Program FEDER2014-2020 Junta de Andalucía-Consejería de Economía y Conocimiento” under project E-FQM-262-UGR18 by Universidad de Granada.

致谢本工作部分得到以下项目资助:NSF-PHY-1903799、NSF-PHY-2206557、赫恩理论物理研究所基金、CCT-LSU、Pedeciba、克莱门特·埃斯特布尔基金 FCE 1 2019 1 155865，以及西班牙政府项目 PID2020-118159GB-C43、PID2019-105943GB-I00(含欧洲区域发展基金资助), 还有格拉纳达大学“安达卢西亚-经济与知识委员会 2014-2020 欧洲区域发展基金运营计划”下的 E-FQM-262-UGR18 项目。

References

参考文献

1. I. Agulló, P. Singh, in Loop Quantum Gravity: The First 30 Years, eds. by A. Ashtekar, J. Pullin (World Scientific, Singapore 2017)

2. J. Friedman, I. Jack, Phys. Rev. D 37, 3495-3504 (1988). https://doi.org/10.1103/physrevd.37.3495 and references therein

3. R. Gambini, J. Pullin, Phys. Rev. Lett. 110(21), 211301 (2013). https://doi.org/10.1103/ PhysRevLett.110.211301, [arXiv:1302.5265 [gr-qc]]

4. R. Gambini, J. Olmedo, J. Pullin, Class. Quant. Grav. 31, 095009 (2014). https://doi.org/10.1088/0264-9381/31/9/095009, [arXiv:1310.5996 [gr-qc]]

5. A. Ashtekar, J. Olmedo, P. Singh, Phys. Rev. Lett. 121, 241301 (2018). [arxiv:1806.00648 [gr-qc]]; Phys. Rev. D 98(12), 126003 (2018). https://doi.org/10.1103/PhysRevD.98.126003, [arXiv:1806.02406 [gr-qc]]

6. P. Cordero, C. Teitelboim, Ann. Phys. 100, 607-631 (1976). https://doi.org/10.1016/0003- 4916(76)90074-9

7. M. Bojowald, R. Swiderski, Class. Quant. Grav. 23, 2129-2154 (2006). https://doi.org/10.1088/0264-9381/23/6/015, [arXiv:gr-qc/0511108 [gr-qc]]

8. J. Olmedo, Universe 2(2), 12 (2016). https://doi.org/10.3390/universe2020012, [arXiv:1606.01429 [gr-qc]]

9. K.V. Kuchař, Phys. Rev. D 50, 3961-3981 (1994). https://doi.org/10.1103/PhysRevD.50.3961, [arXiv:gr-qc/9403003 [gr-qc]]

10. A. Ashtekar, T. Pawlowski, P. Singh, Phys. Rev. Lett. 96, 141301 (2006). https://doi.org/10.1103/PhysRevLett.96.141301 [arXiv:gr-qc/0602086 [gr-qc]]

11. A. Ashtekar, J. Lewandowski, Class. Quant. Grav. 21, R53 (2004). https://doi.org/10.1088/ 0264-9381/21/15/R01, [arXiv:gr-qc/0404018 [gr-qc]]

12. R. Gambini, J. Pullin, Phys. Lett. B 749, 374-375 (2015). https://doi.org/10.1016/j.physletb.2015.08.022, [arXiv:1506.08794 [gr-qc]]

13. R. Gambini, J. Pullin, Universe 6(12), 236 (2020). https://doi.org/10.3390/universe6120236, [arXiv:2010.14519 [quant-ph]]

14. R. Gambini, J. Olmedo, J. Pullin, Class. Quant. Grav. 37(20), 205012 (2020). https://doi.org/10.1088/1361-6382/aba842, [arXiv:2006.01513 [gr-qc]]

15. J. Olmedo, Int. J. Mod. Phys. D 25(08), 1642004 (2016). https://doi.org/10.1142/ S0218271816420049, [arXiv:1604.08129 [gr-qc]]

16. D. Chiou, W. Ni, A. Tang, arXiv:1212.1265

17. R. Gambini, E.M. Capurro, J. Pullin, Phys. Rev. D 91(8), 084006 (2015). https://doi.org/10.1103/PhysRevD.91.084006, [arXiv:1412.6055 [gr-qc]]

18. R. Gambini, J. Olmedo, J. Pullin, Front. Astron. Space Sci. 8, 74 (2021). https://doi.org/10.3389/fspas.2021.647241, [arXiv:2012.14212 [gr-qc]]

19. M. Bojowald, Phys. Rev. D 105(10), 108901 (2022). https://doi.org/10.1103/PhysRevD.105.108901, [arXiv:2203.06049 [gr-qc]]; R. Gambini, J. Olmedo, J. Pullin, Phys. Rev. D 10510, 108902 (2022). https://doi.org/10.1103/PhysRe

20. R. Gambini, J. Olmedo, J. Pullin, Phys. Rev. D 105(2), 2 (2022). https://doi.org/10.1103/ PhysRevD.105.026017, [arXiv:2201.01616 [gr-qc]]

21. N. Arkani-Hamed, L. Motl, A. Nicolis, C. Vafa, JHEP 06, 060 (2007). https://doi.org/10.1088/ 1126-6708/2007/06/060, [arXiv:hep-th/0601001 [hep-th]]

22. N. Wolchover, Black Hole Paradoxes Reveal a Fundamental Link Between Energy and Order, Quanta Magazine (2020)

23. G.T. Horowitz, N. Iqbal, J.E. Santos, B. Way, Class. Quant. Grav. 32, 105001 (2015). https://doi.org/10.1088/0264-9381/32/10/105001, [arXiv:1412.1830 [hep-th]]

24. T. Regge, J.A. Wheeler, Stability of a Schwarzschild singularity. Phys. Rev. 108, 1063-1069 (1957)

25. F.J. Zerilli, Effective potential for even parity Regge-Wheeler gravitational perturbation equations. Phys. Rev. Lett. 24, 737-738 (1970)

26. V. Moncrief, Gravitational perturbations of spherically symmetric systems. I. The exterior problem. Ann. Phys. 88, 323 (1974)

27. S. Chandrasekhar, S.L. Detweiler, The quasi-normal modes of the Schwarzschild black hole. Proc. Roy. Soc. Lond. A 344, 441-452 (1975). https://doi.org/10.1098/rspa.1975.0112

28. S. Iyer, C.M. Will, Black hole normal modes: a WKB approach. 1. Foundations and application of a higher order WKB analysis of potential barrier scattering.I Phys. Rev. D 35, 3621 (1987). https://doi.org/10.1103/PhysRevD.35.3

29. R.A. Konoplya, Quasinormal behavior of the d-dimensional Schwarzschild black hole and higher order WKB approach. Phys. Rev. D 68, 024018 (2003). https://doi.org/10.1103/ PhysRevD.68.024018, [arXiv:gr-qc/0303052]

30. M. Lenzi, C.F. Sopuerta, Darboux covariance: a hidden symmetry of perturbed Schwarzschild black holes. Phys. Rev. D 104, 124068 (2021). [arXiv:2109.00503[gr-qc]]

31. D. del-Corral, J. Olmedo, Breaking of isospectrality of quasinormal modes in nonrotating loop quantum gravity black holes. Phys. Rev. D 105, 064053 (2022). https://doi.org/10.1103/ PhysRevD.105.064053, [arxiv: 2201.09584 [gr-qc]]

32. G. Dotti, R. Gleiser, J. Pullin, Phys. Lett. B 644, 289-293 (2007). https://doi.org/10.1016/j.physletb.2006.12.004, [arXiv:gr-qc/0607052 [gr-qc]]

33. M. Bouhmadi-López, S. Brahma, C.Y. Chen, P. Chen, D.H. Yeom, JCAP 07, 066 (2020). https://doi.org/10.1088/1475-7516/2020/07/066, [arXiv:2004.13061 [gr-qc]]

34. C. Liu, T. Zhu, Q. Wu, K. Jusufi, M. Jamil, M. Azreg-Aïnou, A. Wang, Phys. Rev. D 101(8), 084001 (2020); [erratum: Phys. Rev. D 103(8), 089902 (2021)]. https://doi.org/10.1103/PhysRevD.101.084001, [arXiv:2003.00477 [gr-qc]]

35. A. Ashtekar, M. Bojowald, Class. Quant. Grav. 23, 391-411 (2006)

36. L. Modesto, Class. Quant. Grav. 23, 5587-5602 (2006)

37. C.G. Boehmer, K. Vandersloot, Phys. Rev. D 76, 1004030 (2007)

38. D.W. Chiou, Phys. Rev. D 78, 064040 (2008)

39. M. Assanioussi, L. Mickel, Phys. Rev. D 103, 124008 (2020). [arXiv:2012.06839[gr-qc]]

40. K. Blanchette, S. Das, S. Hergott, S. Rastgoo, Phys. Rev. D 103, 084038 (2021). [arXiv:2011.11815[gr-qc]]

41. D. Cartin, G. Khanna, Phys. Rev. D 73, 104009 (2006)

42. M. Campiglia, R. Gambini, J. Pullin, AIP Conf. Proc. 977(1), 52-63 (2008). https://doi.org/10.1063/1.2902798 [arXiv:0712.0817 [gr-qc]]

43. J. Brannlund, S. Kloster, A. DeBenedictis, Phys. Rev. D 79, 084023 (2009)

44. A. Yonika, G. Khanna, P. Singh, Class. Quant. Grav. 35, 045007 (2018)

45. A. Corichi, P. Singh, Class. Quant. Grav. 33, 055006 (2016)

46. N. Dadhich, A. Joe, P. Singh, Class. Quant. Grav. 32, 185006 (2015)

47. J. Olmedo, S. Saini, P. Singh, Class. Quant. Grav. 34, 225011 (2017)

48. J. Cortez, W. Cuervo, H.A. Morales-Técotl, J.C. Ruelas, Phys. Rev. D 95, 064041 (2017)

49. A. Ashtekar, J. Olmedo, Int. J. Mod. Phys. D 29, 2050076 (2020). [arxiv:2005.02309 [gr-qc]]

50. C. Zhang, Y. Ma, S. Song, X. Zhang, Phys. Rev. D 102, 041502 (2020). [arXiv:2006.08313[gr-qc]]

51. C. Zhang, Y. Ma, S. Song, X. Zhang, Phys. Rev. D 105, 024069 (2021). [arXiv:2107.10579[gr-qc]]

52. B. Elizaga-Navascués, A. García-Quismondo, G.A. Mena-Marugán, [arXiv:2208.00425[gr-qc]]

53. E. Alesci, S. Bahrami, D. Pranzetti, Phys. Lett. B 797, 134908 (2019). [arXiv:2208.00425.[gr-qc]]

54. E. Alesci, S. Bahrami, D. Pranzetti, Phys. Rev. D 102, 066010 (2020). [arXiv:2007.06664.[gr-qc]]

55. W. Gana, G. Ongole, E. Alesci, Y. An, F. Shua, A. Wanga, [arXiv:2206.07127.[gr-qc]]

56. M. Assanioussi, A. Dapor, K. Liegener, Phys. Rev. D 101, 026002 (2020). [arXiv:1908.05756.[gr-qc]]

57. A. Alonso-Bardaji, D. Brizuela, R. Vera, Phys. Rev. D 106, 024035 (2022). [arXiv:2205.02098.[gr-qc]]

58. F. Benitez, R. Gambini, L. Lehner, S. Liebling, J. Pullin, Phys. Rev. Lett. 124, 071301 (2020). [arXiv:2002.04044 [gr-qc]]

59. F. Benitez, R. Gambini, S. Liebling, J. Pullin, Phys. Rev. D 104, 024008 (2021). [arXiv:2106.00674 [gr-qc]]

60. J.G. Kelly, R. Santacruz, E. Wilson-Ewing, Class. Quantum Grav. 38, 04LT01 (2021). [arXiv:2006.09325.[gr-qc]]

61. V. Husain, J.G. Kelly, R. Santacruz, E. Wilson-Ewing, Phys. Rev. D 106, 024014 (2022). [arXiv:2203.04238.[gr-qc]]

62. M. Bouhmadi-López, S. Brahma, C.Y. Chen, P. Chen, D.H. Yeom, Phys. Dark Univ. 30, 100701 (2020). https://doi.org/10.1016/j.dark.2020.100701, [arXiv:1902.07874 [gr-qc]]

63. J. Lewandowski, Y. Ma, J. Yang, C. Zhang, Phys. Rev. Lett. 130(10), 101501 (2023). https://doi.org/10.1103/PhysRevLett.130.101501, [arXiv:2210.02253 [gr-qc]]

64. S. Hossenfelder, L. Modesto, I. Premont-Schwarz, Phys. Rev. D 81, 044036 (2010). https:// doi.org/10.1103/PhysRevD.8
[arXiv:0912.1823 [gr-qc]]; C. Rovelli, F. Vidotto, Int. J. Mod. Phys. D 23(12), 1442026 (2014). https://doi.org/10.1142/S02182718
[arXiv:1401.6562 [gr-qc]]; J. Ziprick, J. Gegenberg, G. Kunstatter, Phys. Rev. D 94(10), 104076 (2016). https://doi.org/10.1103/Ph
[arXiv:1609.06665 [gr-qc]]; K. Giesel, B.F. Li, P. Singh, Phys. Rev. D 104(10), 106017 (2021). https://doi.org/10.1103/PhysRevD.104.106017, [arXiv:2107.05797 [gr-qc]]